BNL-221835-2021-JAAM

Warming and elevated CO2 alter tamarack C fluxes, growth and mortality: evidence for heat stress-related C starvation in the absence of water stress

B. Murphy, D. A. Way

To be published in "Tree Physiology"

May 2021

Environmental and Climate Sciences Department

Brookhaven National Laboratory

U.S. Department of Energy

BNL Program Development

DISCLAIMER

Warming and elevated CO_2 alter tamarack C fluxes, growth and mortality: evidence for heat stress-related C starvation in the absence of water stress

Running Head: Heat stress-induced C limitations in tamarack

Bridget K. Murphy[1*] and Danielle A. Way[1,2,3]

[1] Department of Biology, University of Western Ontario, London, Ontario, Canada

[2] Nicholas School of the Environment, Duke University, Durham, NC, USA

[3] Terrestrial Ecosystem Science & Technology Group, Environmental & Climate Sciences Department, Brookhaven National Laboratory, NY, USA

*Corresponding Author; email: bridget.murphy@mail.utoronto.ca

Article Type: Original Article

Word Count: 6,056

Introduction: 1,251

Methods: 1,604

Results: 763

Discussion: 2,438

Number of Tables: 3

Number of Figures: 9

Supplementary Figures: 1

Abstract

Climate warming is increasing the frequency of climate-induced tree mortality events. While drought combined with heat is considered the primary cause of this mortality, little is known about whether moderately, high temperatures alone can induce mortality, or whether rising CO_2 would prevent mortality at high growth temperatures. We grew tamarack (*Larix laricina)* under ambient (400 ppm) and elevated (750 ppm) CO_2 concentrations combined with ambient, ambient +4 ˚C, and ambient +8 ˚C growth temperatures to investigate whether high growth temperatures lead to carbon limitations and mortality. Growth at +8 ˚C led to 40% mortality in the ambient CO_2 (8TAC) treatment, but no mortality in the elevated CO_2 treatment. Thermal acclimation of respiration led to similar leaf carbon balances across the warming treatments, despite a lack of photosynthetic acclimation. Photosynthesis was stimulated under elevated CO_2, increasing seedling growth, but not leaf carbon concentrations. However, growth and foliar carbon concentrations were lowest in the +8 ˚C treatments, even with elevated CO_2. Dying 8TAC seedlings had lower needle carbon concentrations and lower ratios of photosynthesis to respiration than healthy 8TAC seedlings, indicating that carbon limitations were likely the cause of seedling mortality under high growth temperatures.

Keywords: acclimation, carbohydrates, climate change, J_{max}, non-structural carbohydrates, survival, V_{cmax}

Introduction

With atmospheric CO_2 concentrations increasing at ~2.0 ppm per year, global temperatures are projected to increase 2.0-4.5 ˚C by the year 2100 (Cramer et al. 2014). Warming is most extreme in high northern latitudes, which could experience temperature increases of more than 8 ˚C by the end of the century (Oppenheimer et al. 2014, Serreze et al. 2000). These increased temperatures and atmospheric CO_2 concentrations have already intensified climatic stress on vegetation, leading to greater tree mortality globally. Since 1970, there have been over 88 documented large-scale tree mortality events, and tree mortality has been identified as a major contributor to future vegetation shifts (Allen et al. 2010, Allen et al. 2015). Many forest mortality events have been linked to global change-related droughts, where high temperatures and drought occur simultaneously. Tree die-offs have therefore been largely attributed to water stress causing either hydraulic failure (i.e. catastrophic xylem cavitation) or carbon (C) starvation (where low stomatal conductance suppresses photosynthetic C gains, but respiratory C losses remain high) (Adams et al. 2017, Allen et al. 2010, Anderegg et al. 2012, Hartmann et al. 2018, Mcdowell and Sevanto 2010; Sevanto et al. 2014).

Tree die-offs are already proving to be detrimental to the boreal biome. In high latitude regions in North America, boreal tree species have had mortality rate increases of up to 4.7% per year since 1963 (Peng et al. 2011), likely due to climate change. But while warming was positively correlated with mortality rates for all plots in Peng et al. (2011), water deficits were only positively correlated with mortality rates in western Canada, indicating that temperature, and not drought, may be the main driver of

70 mortality, a finding supported by Luo and Chen (2015). This raises the question of
71 whether warming may directly increase tree mortality risk through carbon starvation,
72 even when water supplies are ample, an idea which has received little attention. High
73 temperatures may cause carbon starvation if they reduce the ratio of photosynthesis to
74 respiration sufficiently such that tree carbon stores are depleted without being
75 replenished. However, if this is true, high CO_2 concentrations predicted over the next
76 few decades may counteract this warming effect by stimulating photosynthesis,
77 meaning that tree mortality rates would not increase under future warming combined
78 with elevated CO_2.

79 Photosynthesis, a key determinant of plant C balance, is sensitive to both CO_2
80 concentrations and temperature. Photosynthesis is stimulated by short-term exposure to
81 high CO_2 concentrations, as ribulose-1,5-bisphosphate carboxylase/oxygenase
82 (Rubisco) is substrate-limited under current CO_2 concentrations (Ainsworth and Rogers
83 2007). Thus, high CO_2 conditions increase substrate availability for photosynthesis and
84 suppress photorespiration (Drake et al. 1997). However, plants will often down-regulate
85 net CO_2 assimilation rates (A_{net}) after long-term exposure to elevated CO_2 to cope with
86 sink limitations related to low nitrogen availability (Ainsworth and Rogers 2007, Tjoelker
87 et al. 1998). In contrast, the temperature response of A_{net} is curvilinear, with A_{net}
88 peaking near the growth temperature experienced by the plant (Sage and Kubien 2007).
89 Above this thermal optimum, A_{net} declines, due to increases in respiration and
90 photorespiration, and often also due to declines in stomatal conductance (Lin et al.
91 2012, Sage and Kubien 2007). Plants acclimate to warming by shifting the
92 photosynthetic temperature optimum towards higher temperatures (Way and Yamori

93 2014). However, thermal acclimation can result in increased, similar or even lower rates
94 of A_{net} at the new growth temperature compared to a control plant (Way and Yamori
95 2014), meaning that even in plants that thermally acclimate, carbon availability may be
96 reduced in warm-grown plants.

97 Photosynthetic capacity, a measure of the maximum capacity of a leaf to fix CO_2,
98 can also be used to quantify photosynthetic thermal acclimation (Way and Yamori
99 2014). Photosynthetic capacity consists of both the maximum rate of electron transport,
100 J_{max}, and the maximum rate of Rubisco carboxylation, V_{cmax}. Elevated growth
101 temperatures and growth CO_2 concentrations both affect J_{max} and V_{cmax}. Plants can
102 decrease their photosynthetic capacity in warm growth conditions to maintain a similar
103 rate of A_{net} as that achieved by cool-grown plants, thus maintaining carbon uptake while
104 reducing leaf N costs (Dusenge et al. 2020). In contrast, an increase in photosynthetic
105 capacity at warmer growth temperatures will maximize A_{net} in conditions where water
106 and nutrient availability are not limiting (Way and Yamori 2014). Thus, both a decrease
107 and an increase in V_{cmax} and J_{max} in warm-grown plants may represent photosynthetic
108 thermal acclimation (Way and Yamori 2014). Photosynthetic capacity can also be
109 affected by growth under elevated CO_2. Long-term exposure of plants to elevated CO_2
110 often results in a decrease in photosynthetic capacity (Ainsworth and Rogers 2007,
111 Albert et al. 2011, Moore et al. 1999). Under elevated CO_2, plants are able to maintain
112 high photosynthetic rates with less investment in Rubisco, since CO_2 substrate
113 availability is high. Leaf N can act as a proxy for Rubisco concentrations (Reich et al.
114 1998), and changes in leaf N concentrations in plants grown at high CO_2 are often used

115 as indicators of changes in photosynthetic capacity (Crous et al. 2008, Kattge et al.
116 2009).

117 The other main determinant of plant C balance is respiration. Over minutes to
118 hours, respiration increases exponentially with increasing temperatures (Atkin and
119 Tjoelker 2003), but respiration is relatively insensitive to short-term changes in CO_2
120 concentrations (Amthor et al. 2001). Under longer-term exposure to elevated
121 temperatures, thermal acclimation of respiration often results in a decrease in
122 respiration at a common measurement temperature, which mitigates plant C losses
123 (Atkin and Tjoelker 2003, Slot and Kitajima 2015). Long-term exposure to elevated CO_2
124 can also increase respiration in both herbaceous and woody species (Davey et al. 2004,
125 Jauregui et al. 2015, Way et al. 2015), though this is not always the case (Haworth et al.
126 2015, Tissue et al. 2002).

127 To avoid C starvation, plants must be able to acclimate both photosynthesis and
128 respiration in a manner that ensures a sufficient supply of carbohydrates for growth and
129 metabolism. If plants are unable to balance the ratio of photosynthesis to respiration
130 under elevated growth temperatures and CO_2 concentrations, they will be at risk for
131 growth reductions and mortality from C starvation in future climate conditions. Tamarack
132 is a deciduous conifer that is widely distributed across North America and contributes to
133 the boreal forest's C sequestration potential. Deciduous conifers are considered to be
134 highly phenotypically plastic as they produce new needles each spring that can
135 maximize photosynthetic capacity (Gower and Richards 1990). However, there are also
136 trade-offs associated with tamarack's growth strategy, such as reduced water-use-

efficiency (Dusenge et al. 2021), that may impact the survival of this species under future climatic stresses.

In this study, we grew tamarack at either ambient or elevated CO_2 concentrations combined with ambient temperatures or a +4 ˚C or +8 ˚C warming treatment to simulate future climate scenarios. In a recent paper from our group, tamarack seedlings had high levels of mortality under 8 ˚C warming when coupled with ambient CO_2 (Dusenge et al. 2020). We hypothesized that carbon starvation caused this high mortality in tamarack, since: 1) seedlings were well-watered; and 2) seedlings grown under the same +8 ˚C temperature regime, but with elevated CO_2, had no mortality. The main objectives of our study were therefore to evaluate: (i) C fluxes, growth and performance of healthy tamarack seedlings across all six treatments; and (ii) C fluxes, growth and performance of dying tamarack seedlings. The overarching goal was to determine if differences in leaf C balance between dying and healthy seedlings grown under elevated temperatures and ample water imply that heat stress from high growth temperatures can directly induce C starvation.

Materials and methods

Experimental design

Tamarack seeds were sown on May 12, 2017 in 11.3 L pots filled with Promix HP mycorrhizal growing medium (Premier Tech Horticulture, Rivieire-du-Loup, QC, Canada) with slow-release fertilizer (Slow Release Plant Food, 12-4-8, Miracle Grow, The Scotts Company, Mississauga, ON, Canada). Seeds were ordered from the Canadian National Seed Tree Center (provenance from Finch Township, ON, 45.133

°N, 75.083 °W) to match the seed collection site with ambient growing season temperatures and photoperiods of London, ON where the experiment was performed. While tamarack grows across the northern latitudes of North America (Brandt 2009), and thus experiences low mean annual temperatures, growing season temperatures are more moderate, with mean maximum August temperatures of 26.2 ˚C over the years 2012-2016 (Environment Canada) for the collection site of the seeds used in this experiment.

Forty pots with five seeds per pot were randomly assigned to each of six climate-controlled glasshouses at the University of Western Ontario's Biotron Experimental Climate Change Research Centre (N = 240 pots). Once seedlings were established, seedlings were thinned to one per pot. Each 6.0 m x 3.4 m x 4.3 m glasshouse had a different temperature X CO_2 treatment. Seedlings were grown under either ambient CO_2 (AC, 400 ppm) or elevated CO_2 (EC, 750 ppm) concentrations with either ambient (0T, ambient control temperatures), ambient +4 ˚C (4T) or ambient +8˚C (8T) day and night temperatures (Figure 1). The temperature treatments were chosen to represent a realistic range of possible future temperatures: mean annual air temperature is expected to warm up to 5.8 ˚C under the Representative Concentration Pathway (RCP) 4.5 and up to 9.0 ˚C under RCP8.5 by 2100 in the Great Lakes Basin (McDermid et al. 2014), where the tamarack seeds used in the experiment were collected. The 0T temperature regime was determined from hourly temperature averages for each day of the growing season (using data from 2012-2016) from the London, ON airport meteorological station (Environment Canada), and varied daily over the experiment accordingly. CO_2 concentrations were measured in each glasshouse every 10 minutes

183 with an infrared gas analyzer in the Argus control system (Argus Control Systems,
184 Surrey, Canada) and were controlled by injecting pure CO_2 as needed to maintain the
185 EC treatment (Figure 1B). The growth irradiance inside the glasshouses is
186 approximately ~35% of outdoor light irradiance (Kurepin et al. 2018), varying with
187 naturally fluctuating sunlight. Humidity was controlled at 60% and seedlings were
188 watered as needed to maintain a moist growth medium (Figure S1).
189 Once seedlings were established and thinned, stem height and health ratings
190 were recorded for all seedlings every 14 days. Health was rated on a scale of 1-5 based
191 on the percent of brown needles (Figure 2). Volumetric soil water content was
192 measured in each pot every 14 days (HH2 Moisture Meter, Delta-T Devices,
193 Cambridge, UK).
194
195 *Physiological measurements*
196 Shoot gas exchange measurements were taken in August and September 2017
197 (when the maximum average daytime air temperature in the 0T treatment was 25 ˚C) on
198 fully-expanded needles using a portable photosynthesis system with the opaque conifer
199 chamber (Li-cor 6400XT and 6400-22L, Li-cor Biosciences, Lincoln, NE) and plasticine
200 was used around the gaskets where stems entered the cuvette to prevent any leakage.
201 First, six healthy seedlings from each treatment were measured to establish treatment
202 effects (N=36). Then, to compare gas exchange across seedlings of varying health, six
203 healthy and six dying (health rating = 2-4) seedlings were measured in the 8TAC
204 treatment. Needles from dying seedlings measured in the opaque conifer chamber
205 included those with variable but minor degrees of browning when necessary.

206 The A_{net} was quantified at a range of intracellular CO_2 concentrations (i.e. A/C_i
207 curves) of 50, 200, 300, 400, 500, 600, 750, 1200, 1600 and 2000 ppm. A/C_i curves
208 were measured at a standard leaf temperature of 25 ˚C for all treatments and at the
209 respective growth temperatures (25 ˚C for AT; 29 ˚C for 4T; 33 ˚C for 8T), where the
210 growth temperature was taken as the mean of the daily maximum air temperature at the
211 beginning of the measurements. The A_{net} was assessed at light saturation (1200 µmol
212 photons m^{-2} s^{-1}) and a relative humidity (RH) of 30-65%. Relative humidity (RH) was
213 held constant at ~65% at the 25 ˚C measurement temperature, however RH decreased
214 with increasing measurement temperature despite the use of an inline humidifier for the
215 photosynthesis system. After the last A/C_i measurement was recorded at 2000 ppm
216 CO_2, the cuvette CO_2 was set to 400 ppm and the sample was dark acclimated for 20
217 minutes. Shoot dark respiration (R_{shoot}) was then measured at 400 ppm in all seedlings,
218 as there is no short-term effect of CO_2 on R_{shoot} (Amthor et al. 2001). The R_{shoot} was
219 measured at 25 ˚C ($R_{shoot-25}$) and 35 ˚C ($R_{shoot-35}$) and these data were used to calculate
220 Q_{10} values, defined as the temperature sensitivity of respiration rates over a 10 ˚C
221 temperature increase (Atkin and Tjoelker 2003), using the approach of Loveys et al.
222 (2003):

$$Q_{10} = \left(\frac{R_{shoot-35}}{R_{shoot-25}}\right). \qquad \textit{(Eq. 1)}$$

223 Using the Q_{10} and $R_{shoot-25}$ values, shoot respiration at the growth temperature ($R_{shoot-growth}$)
224 was calculated for each seedling. Shoot growth temperatures were based on the
225 mean daily maximum air temperature in the treatments at the beginning of the
226 measurements.

Maximum rates of electron transport (J_{1200}) and Rubisco carboxylation (V_{cmax}) were estimated from the A/C_i curves using the Farquhar-von Caemmerer-Berry model of C_3 photosynthesis (Farquhar et al. 1980) as described in Medlyn et al. (2002) and used in the R package 'plantecophys' by Duursma (2015). We used the default values for the K_m (710.3 μmol mol^{-1}, which is given by $K_c (1 + O_i/K_o)$, where K_c and K_o are the Michaelis-Menten constants for Rubisco carboxylation (K_c) and oxygenation (K_o), respectively, and O_i is the intercellular O_2 concentration) and the photorespiratory CO_2 compensation point (Γ*, 42.75 μmol mol^{-1}) in Duursma (2015), and incorporated temperature-corrections for these parameters as determined in Bernacchi et al. (2001). The reported rates of photosynthetic capacity are apparent J_{1200} and apparent V_{cmax}, as mesophyll conductance was not measured (given that approaches for reliably measuring mesophyll conductance in short-needled conifers are lacking), and photosynthetic capacity values were based on data from intracellular CO_2 (C_i) concentrations rather than CO_2 concentrations at the site of carboxylation (C_C).

Once gas exchange measurements were complete, needles in the cuvette were removed and photographed to determine projected leaf area (LA) using ImageJ (US National Institutes of Health, Bestheda, MD, USA). The needles were dried at 65 ˚C for 48 h and weighed for biomass to determine leaf mass area LMA (i.e. needle biomass divided by LA), and then used for carbon and nitrogen analyses.

Biomass

After gas exchange measurements were completed, the remaining four-month old seedlings in the experiment were harvested and dried to a constant mass at 65 ˚C.

All seedlings, including those used for gas exchange, (n=40) were divided into roots, shoots, and leaves, and each tissue was weighed individually.

Carbon and nitrogen analysis

A subset of the dried leaf tissue was ground using a Wiley mill (Thomas Scientific, Swedesboro, NJ, USA) and analyzed for carbon and nitrogen concentrations using an elemental analyzer (NCS 2500, Carlo Ebra, Peypin, France).

Non-structural carbohydrate concentrations (glucose, fructose, sucrose, and starch) were extracted according to Landhäusser et al. (2018). Sugars were extracted from dried, ground needle tissue using 80% ethanol and the residual tissue pellet was used for starch determination. Soluble sugars were determined through the addition of enzymes (glucose hexokinase, GHK, assay reagent for glucose; phosphoglucose isomerase for fructose; and invertase for sucrose; Sigma-Aldrich Co., Saint Louis, MO, USA) to sugar extracts and the absorbance was read at 340 nm after 75 min of incubation on a shaker at room temperature (Versa max microplate reader, Molecular Devices, S/N BN02815, Molecular Devices Corporation, Sunnyvale, CA, USA). Residual tissue pellets were digested through the addition of α-amylase and amyloglucosidase (Sigma-Aldrich). The resulting glucose hydrolysate was converted to glucose with the addition of GHK and the absorbance was read at 340 nm after 75 min of incubation on a shaker at room temperature. Using a standard glucose curve, concentrations of glucose, fructose, sucrose, and starch were determined. In samples where sucrose was undetectable, a value of zero was reported.

Statistics

R software (R Foundation for Statistical Computing, Vienna, Austria, EU) was used for modeling and statistical analyses. The R package 'plantecophys' was used to estimate J_{1200} and V_{cmax} (Duursma 2018). The R package 'tidyverse' was used for all statistical analyses (Wickham 2017). Response variables of healthy seedlings from all six treatments were analyzed using two-way ANOVAs, considering growth temperature, growth CO_2 and their interaction. Orthogonal polynomial contrasts were specified for the three levels of the temperature variable and thus type III sum of squares were used for the model. The R package 'nlme' was used to compute type III ANOVA tests (Pinheiro et al. 2013). Log transformation was used to normalize the biomass and height data before the two-way ANOVA was performed. A *post-hoc* Tukey test was used when significant treatment effects were found. The R package 'emmeans' was used to compute *post-hoc* tests (Lenth et al. 2021). The comparison of variables between healthy and dying 8TAC seedlings was done with a two-sample t-test. The treatments were each imposed in a single greenhouse, raising the concern of pseudoreplication. However, our study builds on an earlier study from our group (Dusenge et al. 2020) that grew the same species in these glasshouses and treatments in a separate year, and similarities in the results of common measurements between the two studies (e.g. dark respiration rates at a common temperature, Q_{10}, and growth patterns across the treatments) provide confidence that our conclusions are robust.

Results

Temperature and CO_2 Effects on Healthy Tamarack Seedlings

Carbon fluxes and photosynthetic capacity

When comparing A_{net} under common conditions of 400 ppm CO_2 and 25 ˚C (A_{25}), there was no difference in A_{25} across the treatments (Figure 3A, Table 1). Under these common measurement conditions, there was also no significant treatment effect on stomatal conductance (g_{s25}), the ratio of intracellular CO_2 to ambient CO_2 (C_i/C_{a25}), or transpiration (E_{25}; Tables 1 and 2). The $R_{shoot\text{-}25}$ decreased with increasing growth temperature, but the Q_{10} of shoot respiration was not significantly altered by the treatments (Figure 3B, Tables 1 and 2). The ratio of A_{25} to $R_{shoot\text{-}25}$ (A/R_{25}), an index of shoot-level C balance, therefore increased with increasing growth temperature, but there was no evidence for a CO_2 effect on A/R_{25} (Figure 3C, Table 1).

In contrast, A_{net} measured at the growth CO_2 and temperature (A_{growth}) was 49-69% higher in EC seedlings compared to AC plants, although A_{growth} showed no significant response to growth temperature (Figure 3D, Table 1). Stomatal conductance at growth conditions ($g_{s\text{-}growth}$) showed little response to the treatments, while transpiration measured at growth conditions (E_{growth}) increased with warming and the higher measurement vapour pressure deficit (VPD, i.e., the difference in vapour pressure inside and outside of the leaf) associated with high measurement temperatures (Tables 1 and 2). The ratio of intracellular CO_2 to ambient CO_2 at growth conditions ($C_i/C_{a\text{-}growth}$) was higher in EC than AC seedlings (Tables 1 and 2). Shoot dark respiration rates at growth temperature ($R_{shoot\text{-}growth}$) showed little response to either growth temperature or CO_2 (Figure 3E, Table 1). The ratio of A_{growth} to R_{growth} (A/R_{growth}) was stimulated by EC (Figure 3F, Table 1).

When measured at 25 ˚C, the maximum rate of Rubisco carboxylation ($V_{cmax-25}$) and the maximum rate of electron transport ($J_{1200-25}$) were not significantly affected by the treatments (Figures 4A and B, Table 1). The ratio of $J_{1200-25}/V_{cmax-25}$ decreased from 0T to 8T, and increased with EC (Figure 4C, Table 1). When measured at the growth conditions, the maximum rate of Rubisco carboxylation ($V_{cmax-growth}$) was increased by warming (Figure 4D, Table 1), but the maximum rate of electron transport ($J_{1200-growth}$) was not significantly affected by the treatments (Figure 4E, Table 1). The ratio of $J_{1200-growth}/V_{cmax-growth}$ therefore decreased with warming and also increased with EC (Figure 4F, Table 1).

Growth response

Seedling growth was affected by both growth temperature and CO_2 (Figure 5, Table 1). As growth temperature increased from 0T to 4T, total seedling biomass was constant, but biomass decreased at 8T (Figure 5E, Table 1). There was also greater biomass in EC compared to AC seedlings. The ratio of root/shoot biomass was similar across the warming treatments in AC seedlings, but higher in 8T than 0T in EC seedlings due to increased root biomass (Figures 5B and C, Table 1). Tree height was increased by EC only in the 0T seedlings, and 8T seedlings were shorter than 0T and 4T plants in both CO_2 treatments (Figure 5F, Table 1).

Tissue biochemistry

Leaf %N was lower in EC than AC seedlings, but there was little effect of growth temperature on leaf %N (Figure 6A, Table 1). In contrast, as growth temperature

increased, needle %C declined, with no apparent effect of growth CO_2 on leaf %C (Figure 6B, Table 1). The ratio of C/N was increased by EC but did not respond to growth temperature (Figure 6C, Table 1). Needle soluble sugar and total non-structural carbohydrate concentrations decreased with warming but were not significantly affected by growth CO_2 (Figures 6D and F, Table 1), while needle starch concentrations were similar across all treatments (Figure 6E, Table 1).

Comparison of Dying vs. Healthy Seedlings in the 8TAC Treatment

Overall, 8TAC seedlings had a 40% mortality rate compared to 0% mortality in all other treatments. Similar to the quantification of C fluxes of healthy seedlings across all treatments, the same traits were examined in 8TAC dying and healthy seedlings at their growth temperature of 33 ˚C. There was no significant difference in A_{growth}, $R_{shoot\text{-}growth}$, $J_{1200\text{-}growth}$, $V_{cmax\text{-}growth}$ or $J_{1200}/V_{cmax\text{-}growth}$ between healthy and dying seedlings, nor was there any significant difference in the ratio of A_{growth} to $R_{shoot\text{-}growth}$ (A/R_{growth}) (Figures 7A-F, Table 3). Needle %C was lower in the dying seedlings, although the needle %N and the ratio of C/N were similar between all 8TAC seedlings (Figures 8A-C, Table 3). Non-structural carbohydrate concentrations were also similar across the two groups of seedlings (Figures 8D-F, Table 3). However, there were significant negative correlations between the health rating of the seedlings and both the needle %C and the ratio of A/R_{growth} (Figures 9A and B).

Discussion

Carbon balance and photosynthetic capacity

There was surprisingly little evidence for photosynthetic acclimation across 8 ˚C of warming and a 350 ppm increase in growth CO_2, indicating that tamarack has considerable capacity for maintaining C uptake under future climates. Many studies have shown that plants grown at elevated CO_2 tend to have reduced photosynthetic capacity (Ainsworth and Long 2005, Albert et al. 2011, Moore et al. 1999), but our data support the idea that conifers may be less sensitive to rising CO_2 than other plant functional types (Ainsworth and Rogers 2007, Medlyn et al. 2001, Ellsworth 1999). While less is known about how deciduous conifers will respond to elevated CO_2 compared to evergreen conifers, Dusenge et al. (2020) also found that photosynthetic capacity was unresponsive to changing CO_2 in tamarack seedlings.

Photosynthetic acclimation to temperature is also common in the literature (Kroner and Way 2016, Tjoelker et al. 1998, Way and Oren 2010, Yamori et al. 2014, Yamori et al. 2005). However, the response of A_{net} to warming is variable in boreal tree species. Previous studies have found that *Picea asperata, Abies faxoniana* and *Pinus sylvestrius* seedlings increase A_{growth} with warming, whereas *Picea abies* and *Picea mariana* seedlings decrease A_{growth} with warming (Kurepin et al. 2018, Tjoelker et al. 1998, Yin et al. 2008). While it is unusual to find the degree of photosynthetic stability across such a broad range of growth temperatures as seen in our data, thermal acclimation can result in a similar A_{growth} across different growth temperatures (Way et al. 2014). Stomatal conductance was also constant across the warming treatments, which may have contributed to the similar A_{growth} observed here. Despite high growth temperatures at 8T, the volumetric water content maintained in the soil would have allowed the seedlings to maintain similar rates of photosynthesis and transpiration

compared to the 0T and 4T warming treatments. The lack of photosynthetic acclimation was also correlated with the maintenance of relatively similar concentrations of needle N, implying that warming had little effect on photosynthetic enzyme and protein concentrations across the treatments.

Since g_s was also relatively insensitive to warming and CO_2, there was higher $C_i/C_{a\text{-}growth}$ under EC, and therefore higher A_{growth} in the EC seedlings. At current CO_2 concentrations, Rubisco is substrate-limited; by increasing intracellular CO_2 concentrations, photosynthetic rates increase and photorespiration is suppressed (Sage and Kubien 2007). Stimulation of photosynthesis by EC in mature conifers is common in the absence of sink limitations (Ainsworth and Rogers 2007, DeLucia et al. 1999, Dusenge et al. 2020, Ryan 2013), as these limitations can feed back to instigate a down-regulation of photosynthesis (Ainsworth and Long 2005, Leakey et al. 2009). Dusenge et al. (2020) and Tjoelker et al. (1999a) also found that warming led to a constant A_{growth}, but that EC stimulated A_{growth} in tamarack, indicating that photosynthetic rates of tamarack are highly responsive to changes in elevated CO_2, even when stomatal conductance is not.

While photosynthetic capacity at 25 ˚C was unaffected by the treatments, the ratio of $J_{1200\text{-}25}$:$V_{cmax\text{-}25}$ was slightly reduced with warming. Meta-analyses have noted that the effect of warming on photosynthetic capacity measured at 25 ˚C is variable (Way and Oren 2010; Way et al. 2014), and we still lack a general understanding of how $V_{cmax\text{-}25}$ and $J_{1200\text{-}25}$ will be affected by a warming world. Tamarack seedlings in Dusenge et al. (2020) had decreased photosynthetic capacity with warming and associated decreases in foliar nitrogen concentrations (%N), indicative of a lower

investment in photosynthetic enzymes (Reich et al. 1998). Comparatively, in our data, photosynthetic capacity did not acclimate to warming and there was a similar %N across temperature treatments, indicating there was likely no large change in the relative amounts of Rubisco across the treatments. But the decline in $J_{1200\text{-}25}$:$V_{cmax\text{-}25}$ in warm-grown plants is common (Kattge and Knorr 2007, Yamori et al. 2005, Dusenge et al. 2020), and is thought to indicate a shift in nitrogen partitioning within the photosynthetic apparatus from RuBP carboxylation to RuBP regeneration (Hikosaka et al. 2006). Under low temperatures, plants invest more nitrogen into RuBP regeneration, resulting in a higher ratio of cytochrome *f* to rubisco and subsequently a higher ratio of $J_{1200\text{-}25}$:$V_{cmax\text{-}25.}$(Onada et al. 2005), with the opposite occurring at warm temperatures. The shift in $J_{1200\text{-}25}$:$V_{cmax\text{-}25}$ found here was small, though significant, implying that there may have been subtle shifts in N allocation between electron transport and carboxylation capacity across the treatments.

When measured at growth conditions, $J_{1200\text{-}growth}$ was constant across the treatments, while $V_{cmax\text{-}growth}$ increased from 0T to 8T. Rising leaf temperatures generally stimulate both V_{cmax} and J_{1200} (Kattge and Knorr 2007, Way and Oren 2010), which makes the J_{1200} data somewhat surprising. However, the “co-ordination hypothesis” predicts that V_{cmax} and J_{max} should be co-limiting (Hikosaka et al. 2006, Maire et al. 2012, Togashi et al. 2018). Given this, the stimulation of $V_{cmax\text{-}growth}$ with warming may allow plants to match higher Rubisco activity with higher photosynthetic rates (Togashi et al. 2018). Higher rates of RuBP carboxylation by Rubisco would maintain A_{growth} across the warming treatments despite the greater photorespiratory losses expected with increased temperatures. Both $J_{1200\text{-}25}$:$V_{cmax\text{-}25}$ and $J_{1200\text{-}growth}$:$V_{cmax\text{-}growth}$ increased in

EC seedlings, a result linked to increased efficiency of Rubisco carboxylation under high CO_2 and a resultant rebalancing of allocation towards J_{1200} (Crous et al. 2008).

Thermal acclimation of respiration mitigated C losses across the warming treatments, as seen in other studies (Atkin and Tjoelker 2003, Dusenge et al. 2020, Loveys et al. 2003, Reich et al. 1998, Slot and Kitajima 2015, Tjoelker et al. 1999a). Overall, thermal acclimation of respiration led to similar rates of R_{growth} and similar $A:R_{growth}$ from 0T to 8T. In comparison, photosynthetic stimulation by EC increased $A:R_{growth}$. By acclimating respiration, tamarack was able to effectively minimize C losses under +8 ˚C and maintain similar leaf C balances in healthy seedlings across all warming treatments.

Growth, biomass allocation and C/N dynamics

While the leaf C flux data were not indicative of warming stress, tree biomass and height decreased at 8T compared to 0T and 4T (a growth result similar to that in our earlier study of Dusenge et al. 2020). These growth reductions were largely offset by EC, implying that the decline in growth is related to plant C dynamics. In support of this hypothesis, 8TAC seedlings had lower root:shoot ratios than 8TEC seedlings, indicating increased allocation to aboveground tissues (i.e. photosynthetic tissue) to compensate for limited C availability (Poorter et al. 2012). The biomass allocation patterns of different conifer species to warming and EC are variable (Yin et al. 2008). But other work has confirmed that tamarack and other tree species increase allocation to leaf tissue under warming (Dusenge et al. 2020, Way and Oren 2010). Plants with low belowground biomass allocation prioritize C gain over water uptake, which is

456 beneficial under C stress conditions, but could put these trees at greater risk under drier
457 climates in the future (Way and Oren 2010). As tamarack seedlings in this study were
458 well watered and fertilized, 8TAC seedlings were able to invest in aboveground tissues
459 to maximize C gains without experiencing water or nutrient stress, but this may not be
460 true for tamarack that experience warming in the field over coming decades.
461 Warming also reduced foliar C concentrations (%C). Foliar %C has been
462 estimated at ~50% in conifers (Ma et al. 2018), so a reduction by 5% in 8T seedlings is
463 considerable and one indication of C limitation. Surprisingly, these decreases in %C
464 were not offset by EC, a pattern also seen in Tjoelker et al. (1999a). The changes in leaf
465 %C were mirrored by changes in foliar soluble sugar and total non-structural
466 carbohydrate (NSC) concentrations, providing further evidence that warming may have
467 led to a decline in whole tree C balance (Dietze et al. 2014). A meta-analysis by Du et
468 al. (2020) also noted a reduction in soluble sugar concentrations in plants exposed to
469 warmer temperatures. Decreased starch concentrations are also often prevalent under
470 C stress (Du et al. 2020, Sevanto et al. 2014, Wiley et al. 2017) though this was not
471 apparent in the tamarack in our study. Higher C availability from stimulated A_{growth} under
472 EC was apparently allocated to growth over storage, given the strong effect of EC on
473 plant growth. Prioritization of growth over storage is common in conifer seedlings
474 (Dietze et al. 2014), but the small C stores often found in seedlings may make them
475 more vulnerable to C stress under this C allocation strategy.
476 Rising CO_2 concentrations can affect foliar nitrogen content (%N) through a direct
477 suppression of Rubisco production (Crous et al. 2008) or a growth dilution effect (Taub
478 and Wang 2008). A synthesis of 62 plant species by Yin (2002) found that the

479 proportional decline in %N with EC is highest in deciduous woody species, like
480 tamarack. While our EC seedlings had lower leaf %N than the AC tamarack, EC also
481 led to higher A_{growth} as these seedlings were able to invest less in photosynthetic
482 enzymes and still attain higher photosynthetic rates than AC plants. Elevated CO_2 in
483 future climates will likely be beneficial for tamarack C gain and growth, even when
484 combined with moderate warming, as seen here in 0TEC and 4TEC seedlings.
485
486 *Mortality in 8TAC Seedlings*
487 One of the main objectives of this study was to investigate whether C starvation
488 was the cause of mortality in 8TAC seedlings. The few studies that have measured tree
489 mortality have found higher respiration in seedlings experiencing C starvation (Sevanto
490 et al. 2014, Wiley et al. 2017). These studies also found depletions in plant C after long
491 durations of C stress. While we found no significant difference in respiration (or
492 photosynthetic) rates between healthy and dying seedlings, leaf %C was lower in dying
493 8TAC seedlings compared to healthy seedlings, providing evidence of C limitations, and
494 there was a trend ($p=0.08$) towards lower total non-structural carbohydrate
495 concentrations in the dying 8TAC seedlings**.** Additionally, both the ratio of $A:R_{growth}$ and
496 leaf %C were negatively correlated with the health ratings, providing evidence that C
497 balance was depleted as seedling health deteriorated. In measuring healthy 8TAC
498 seedlings, it is important to consider that a survivor effect (i.e. that we only measured
499 healthy seedlings that had survived the treatment) may have biased our estimates of C
500 fluxes, however, this would indicate that our 8TAC C balance results were conservative,
501 given that seedlings that had already died likely had lower photosynthetic rates, higher

502 respiration rates, and lower C stores than the surviving seedlings we sampled. While
503 differences between the mean values of these parameters for the healthy and dying
504 seedlings may also have been obscured by large variation in individual seedlings
505 (especially because dying seedlings were drawn from three different health ratings), our
506 data imply that warming, even without water stress, can lead to C stress and tree
507 mortality.

508 Despite maintaining constant air humidity and volumetric soil water content,
509 some atmospheric water stress may have occurred under +8 ˚C warming, as the VPD
510 would have been ~0.7 kPa higher in the 8T glasshouses than the 0T glasshouse. Given
511 that g_s was unresponsive to warming, this higher VPD in the 8T treatments would lead
512 to higher rates of transpiration in 8T seedlings than those from 0T. This was unlikely to
513 have led to significant water stress in the 8T plants, since they were watered daily and
514 had large soil volumes to hold water compared to their very small root masses. With
515 future warming, relative humidity is expected to stay constant, but as temperatures
516 increase, so will VPD (Dessler and Sherwood 2009, Trenberth 2011, Zhang et al. 2017).
517 Under these ecologically realistic conditions, an inability to acclimate stomatal
518 conductance to warming may be detrimental to tamarack as droughts become more
519 frequent with climate change.

520 The benefits that tamarack and other larch species experience from a deciduous
521 leaf economic strategy, i.e. higher photosynthetic rates, come at a cost compared to the
522 conservative evergreen leaf economic strategy (Kloeppel et al. 2000). The prioritization
523 of C allocation to growth over storage in deciduous conifers results in higher respiratory
524 losses (Tjoelker et al. 1999a) and smaller initial seasonal NSC stores compared to co-

525 occurring evergreens (Hoch et al. 2003). However, over a growing season, NSC pools
526 of deciduous conifers can become similar or even greater than some evergreen conifer
527 species (Tjoelker et al. 1999b), The consequence of initially smaller C stores and higher
528 respiratory costs is that deciduous conifers may have a smaller buffer against climatic
529 stresses that limit photosynthesis and thus may only be able to withstand short periods
530 of C limitation before survival is impacted. Evergreen conifers are considered to be
531 more conservative, with a greater allocation to C storage under stress (Weber et al.
532 2019) and higher water use efficiencies (Soh et al. 2019), which may increase their
533 likelihood of survival. For example, the study from our group that first noted tamarack
534 mortality under 8TAC observed no mortality in black spruce (*Picea mariana)* grown
535 under the same experimental treatments (Dusenge et al. 2020). In addition to plant
536 functional types, intraspecific variation will also impact the future composition of the
537 boreal forest. While population variation in tamarack in response to drought or heat
538 stress has not been well studied, mature white spruce (*Picea glauca*) has increased
539 resilience to drought in populations from drier geographical locations compared to those
540 from more humid locations (Depardieu et al., 2020). Adaptive genetic variation will likely
541 be a strong determinant for thermal plasticity and survival, and it would be useful to
542 compare different genotypic responses of tamarack populations to climatic stresses in
543 future studies.
544
545 *Conclusions*
546 Reduced growth and high mortality were linked to decreases in leaf %C and the
547 balance between photosynthesis and respiration in tamarack seedlings grown under +8

˚C warming coupled with ambient CO_2. In healthy seedlings, thermal acclimation of respiration minimized C losses under warming, resulting in similar leaf C balances across the temperature treatments. While moderate warming (i.e. +4 ˚C) combined with EC may be beneficial to tamarack seedling growth, +8 ˚C warming was detrimental to growth even when combined with EC. To reach a warming of +8 ˚C in high latitudes, atmospheric levels of CO_2 will have to rise, which should help prevent the high mortality observed in our 8TAC seedlings. Additionally, trees in the field may be better equipped than seedlings against high growth temperature-induced C stress as they have larger C stores, which is one of the greatest determinants of survival against C starvation (Hartmann and Trumbore 2016). Regardless, our results indicate that high temperature-induced C stress can ultimately lead to reduced growth and mortality in the absence of water stress, which may be detrimental to the future functioning of tamarack and potentially other boreal tree species as warming continues.

Acknowledgements

We thank Kristyn Bennett for assistance with samples, and Carrie Hamilton and Steve Bartlett for setting up and monitoring the glasshouses. We also thank the National Tree Seed Center for providing seeds for this experiment. B.K.M. was supported by the Queen Elizabeth II Graduate Scholarship for Science and Technology. D.A.W. acknowledges the support of a Natural Sciences and Engineering Research Council of Canada Discovery Grant, support from the Canadian Foundation for Innovation, an Ontario Early Researcher Award, and the United States Department of Energy contract No. DE-SC0012704 to Brookhaven National Laboratory.

Tables

Table 1. Summary of ANOVA statistics for response of gas exchange parameters measured at 25 ˚C and 400 ppm CO_2 (denoted by "25") and at growth conditions (denoted by "growth"), as well as leaf biochemistry and growth, to the treatments. Parameters include: net CO_2 assimilation rate (A_{25}, A_{growth}); shoot dark respiration rate ($R_{shoot\text{-}25}$, $R_{shoot\text{-}growth}$); the ratio of net CO_2 assimilation rate to shoot dark respiration rate (A/R_{25}, A/R_{growth}); the Q_{10} of shoot respiration ($Q_{10\text{-}Rshoot}$); stomatal conductance ($g_{s\text{-}25}$, $g_{s\text{-}growth}$); the ratio of intracellular to ambient CO_2 ($C_i/C_{a\text{-}25}$, $C_i/C_{a\text{-}growth}$); transpiration rate (E_{25}, E_{growth}); the maximum rate of Rubisco carboxylation ($V_{cmax\text{-}25}$, $V_{cmax\text{-}growth}$); the maximum rate of electron transport ($J_{1200\text{-}25}$, $J_{1200\text{-}growth}$); and the ratio of J_{1200} to V_{cmax} ($J_{1200\text{-}25}/V_{cmax\text{-}25}$, $J_{1200\text{-}growth}/V_{cmax\text{-}growth}$); needle percent carbon (%C); needle percent nitrogen (%N); the ratio of C/N; needle soluble sugar concentrations; needle starch concentrations; needle total non-structural carbohydrate (TNC) concentrations; total biomass ($Biomass_{Total}$); leaf biomass ($Biomass_{Leaf}$); stem biomass ($Biomass_{Stem}$); root biomass ($Biomass_{Root}$); the root/shoot ratio ($Biomass_{Root/Shoot}$); and tree height. T = growth temperature, CO_2 = growth CO_2 concentration, CO_2 x T = interaction between growth temperature and CO_2 concentration. *P*-values that are statistically significant ($P \leq 0.05$) are bolded.

	T		**CO_2**		**CO_2 x T**	
	F-Ratio	*P*-value	*F*-Ratio	*P*-value	*F*-Ratio	*P*-value
(A) Gas Exchange Parameters						
A_{25}	0.05	0.95	0.05	0.83	0.21	0.81
$R_{shoot\text{-}25}$	7.09	**<0.05**	1.27	0.27	0.11	0.89
A/R_{25}	4.05	**<0.05**	1.54	0.22	0.04	0.96
A_{growth}	2.90	0.07	52.81	**<0.0001**	1.58	0.22

$R_{shoot\text{-}growth}$	0.18	0.84	2.17	0.15	0.59	0.56
A/R_{growth}	1.16	0.22	9.48	**<0.01**	1.02	0.37
$Q_{10\text{-}Rshoot}$	1.38	0.27	0.001	0.98	3.18	0.06
$g_{s\text{-}25}$	0.02	0.98	0.84	0.37	0.80	0.46
$g_{s\text{-}growth}$	0.37	0.70	0.09	0.77	1.78	0.19
$C_i/C_{a\text{-}25}$	0.29	0.75	0.34	0.56	0.013	0.99
$C_i/C_{a\text{-}growth}$	0.27	0.76	7.67	**<0.01**	0.15	0.86
E_{25}	0.01	0.99	0.20	0.66	0.26	0.77
E_{growth}	6.64	**<0.01**	0.17	0.68	0.71	0.50
(B) Photosynthetic Capacity						
$V_{cmax\text{-}25}$	0.10	0.90	0.12	0.73	0.08	0.92
$J_{1200\text{-}25}$	0.52	0.60	0.86	0.36	0.07	0.93
$J_{1200\text{-}25}/V_{cmax\text{-}25}$	4.65	**<0.05**	29.85	**<0.0001**	0.07	0.93
$V_{cmax\text{-}growth}$	13.30	**<0.0001**	0.59	0.45	0.05	0.95
$J_{1200\text{-}growth}$	0.56	0.58	0.30	0.59	1.07	0.35
$J_{1200\text{-}growth}/V_{cmax\text{-}growth}$	280.60	**<0.0001**	8.14	**<0.001**	13.15	**<0.0001**
(C) Leaf biochemistry						
%N	2.98	0.06	8.54	**<0.01**	2.09	0.14
%C	8.61	**<0.01**	1.48	0.23	0.65	0.53
C/N	1.58	0.22	10.02	**<0.01**	2.12	0.14
Soluble Sugars	4.01	**<0.05**	0.70	0.41	1.54	0.23
Starch	0.19	0.83	0.07	0.79	1.50	0.24
TNC	3.71	**<0.05**	0.59	0.45	1.70	0.20
(D) Growth						
$Biomass_{Total}$	18.75	**<0.0001**	9.57	**<0.01**	0.94	0.39
$Biomass_{Leaf}$	20.33	**<0.0001**	8.94	<**0.01**	0.30	0.74
$Biomass_{Stem}$	24.68	**<0.0001**	9.51	**<0.01**	0.87	0.42
$Biomass_{Root}$	14.38	**<0.0001**	9.87	**<0.01**	2.30	0.10
$Biomass_{Root/Shoot}$	2.15	0.12	6.47	**<0.05**	7.22	**<0.0001**
Tree Height	52.15	**<0.0001**	8.47	**<0.01**	4.45	**<0.05**

589

590

591

Table 2. Response of gas exchange parameters measured at 25 ˚C and 400 ppm CO_2 (denoted by "25") and under growth conditions (denoted by "growth") to the treatments. Parameters include: stomatal conductance ($g_{s\text{-}25}$, $g_{s\text{-}growth}$; mmol H_2O m^{-2} s^{-1}); the ratio of intracellular to atmospheric CO_2 ($C_i/C_{a\text{-}25}$, $C_i/C_{a\text{-}growth}$); transpiration rate (E_{25}, E_{growth}; mmol H_2O m^{-2} s^{-1}); and Q_{10} values of shoot respiration of seedlings from different growth treatments. 0TAC, ambient temperature combined with ambient CO_2; 4TAC, +4 ˚C warming combined with ambient CO_2; 8TAC, +8 ˚C warming combined with ambient CO_2; 0TEC, ambient temperature combined with elevated CO_2; 4TEC, +4 ˚C warming combined with elevated CO_2; 8TEC, +8 ˚C warming combined with elevated CO_2. Means ± SE, n = 6. There were no differences between groups across all six growth treatments, so letters were not used to denote significant differences.

	0TAC	4TAC	8TAC	0TEC	4TEC	8TEC
$g_{s\text{-}25}$	0.16±0.02	0.15±0.01	0.15±0.02	0.15±0.01	0.16±0.01	0.17±0.01
$g_{s\text{-}growth}$	0.16±0.02	0.15±0.01	0.14±0.02	0.14±0.01	0.15±0.01	0.17±0.01
$C_i/C_{a\text{-}25}$	0.76±0.01	0.76±0.01	0.75±0.02	0.76±0.02	0.77±0.01	0.76±0.02
$C_i/C_{a\text{-}growth}$	0.76±0.01	0.74±0.01	0.74±0.02	0.78±0.02	0.78±0.01	0.78±0.02
E_{25}	1.97±0.24	1.81±0.17	1.86±0.26	1.89±0.07	2.00±0.13	1.97±0.19
E_{growth}	1.97±0.24	2.34±0.15	2.76±0.25	2.02±0.12	2.65±0.17	2.61±0.21
Q_{10}	1.70±0.06	1.71±0.02	1.70±0.02	1.63±0.02	1.71±0.05	1.80±0.05

Table 3. Summary of two-sample t-test statistics for parameters comparing dying and healthy 8TAC seedlings: net photosynthesis at growth conditions (A_{growth}); shoot dark respiration at growth conditions ($R_{shoot\text{-}growth}$); ratio between A_{growth} and $R_{shoot\text{-}growth}$ (A/R_{growth}); maximum rate of electron transport (J_{1200}); maximum rate of Rubisco carboxylation (V_{cmax}); ratio between $J_{1200\text{-}growth}$ and $V_{cmax\text{-}growth}$ ($J_{1200}/V_{cmax\text{-}growth}$); percent needle carbon (%C); percent needle nitrogen (%N); the ratio of needle C/N; needle soluble sugar concentrations; needle starch concentrations; and needle total non-structural carbohydrate (TNC) concentrations. DF = degrees of freedom. *P*-values that are statistically significant ($P < 0.05$) are bolded.

	Healthy vs. Dying		
	DF	*T*-stat	*P*-value
A_{growth}	10	0.35	0.73
$R_{shoot\text{-}growth}$	10	0.64	0.54
A/R_{growth}	10	1.87	0.09
V_{cmax}	10	0.60	0.56
J_{1200}	10	1.11	0.30
J_{1200}/V_{cmax}	10	0.62	0.55
% Nitrogen	10	1.30	0.22
% Carbon	10	2.45	**<0.05**
C/N	10	0.91	0.38
Soluble Sugar	10	1.74	0.11
Starch	10	0.64	0.54
TNC	10	1.98	0.08

Figure Captions

Figure 1. Daily temperature and CO_2 levels across all six glasshouses over the duration of the experiment. Day 0 indicates when seeds were potted (May 12th) and day 140 indicates when seedlings were harvested (Sept 28th). Temperature and CO_2 readings were taken daily at 12:00 am. Circles, ambient temperature (0T); triangles, +4 ˚C warming (4T); squares, +8 ˚C warming (8T). White symbols, ambient growth CO_2 (AC); black symbols, elevated growth CO_2 (EC).

Figure 2. Representative seedlings showing the seedling health scale. (1) Needles are 100% green; (2) seedling has <50% brown needle tissue; (3) seedling has approximately 1:1 brown to green leaf tissue; (4) seedling has >50% brown needle tissue; (5) seedling is 100% brown.

Figure 3. Thermal acclimation of respiration led to similar leaf carbon balances across the warming treatments, despite a lack of photosynthetic acclimation in healthy seedlings. Photosynthetic and respiratory responses to elevated CO_2 and temperature treatments measured at 25 ˚C and 400 ppm CO_2 (presented on the left) and growth conditions (25 ˚C for 0T, 29 ˚C for 4T, 33 ˚C for 8T; 400 ppm CO_2 for AC, 750 ppm CO_2 for EC) (presented on the right). **A, D**) net CO_2 assimilation rate ($A_{25^{\circ}C}$, A_{growth}); **B, E**) shoot dark respiration rate ($R_{shoot\text{-}25^{\circ}C,}$ $R_{shoot\text{-}growth}$); **C, F**) the ratio of net CO_2 assimilation rate to respiration rate ($A/R_{25^{\circ}C}$, A/R_{growth}). White, 0T; light grey, 4T; dark grey, 8T. The horizontal line of the boxplot represents the mean; the box edges indicate the 25th and 75th percentiles; the whiskers display the minimum and maximum values; n = 6.

650 Different letters above boxplots denote a significant difference between treatments ($P <$
651 0.05). T = growth temperature, CO_2 = growth CO_2 concentration, n/s = non-significant, *
652 = $P \leq 0.05$, ** = $P<0.01$, and *** = $P<0.001$.
653
654 **Figure 4.** Photosynthetic capacity did not acclimate to either elevated CO_2 or warming in
655 healthy seedlings. Responses of photosynthetic capacity at 25 ˚C and 400 ppm CO_2
656 (presented on the left) and growth conditions (25 ˚C for 0T, 29 ˚C for 4T, 33 ˚C for 8T;
657 400 ppm CO_2 for AC, 750 ppm CO_2 for EC) (presented on the right) to treatments. **A, D**)
658 maximum rate of Rubisco carboxylation ($V_{cmax-25}$, $V_{cmax-growth}$); **B, E**) maximum rate of
659 electron transport ($J_{1200-25}$, $J_{1200-growth}$); **C, F**) the ratio of J_{1200} to V_{cmax} ($J_{1200-25}/V_{cmax-25}$,
660 $J_{1200-growth}/V_{cmax-growth}$). White, 0T; light grey, 4T; dark grey, 8T. The horizontal line of the
661 boxplot represents the mean; the box edges indicate the 25th and 75th percentiles; the
662 whiskers display the minimum and maximum values; n = 6. Different letters above
663 boxplots denote significant differences across all treatments ($P < 0.05$). T = growth
664 temperature, CO_2 = growth CO_2 concentration, n/s = non-significant, * = $P \leq 0.05$, ** =
665 $P<0.01$, and *** = $P<0.001$.
666
667 **Figure 5.** Warming suppressed seedling growth while high CO_2 stimulated growth in
668 healthy seedlings. Growth responses to treatments: **A**) leaf biomass; **B)** root biomass;
669 **C)** the root/shoot ratio; **D)** stem biomass; **E)** total biomass; and **F)** tree height. White,
670 0T; light grey, 4T; dark grey, 8T. The horizontal line of the boxplot represents the mean;
671 the box edges indicate the 25th and 75th percentiles; the whiskers display the minimum
672 and maximum values; n = 40. Different letters above boxplots denote significant

673 differences across all treatments ($P < 0.05$). T = growth temperature, CO_2 = growth CO_2
674 concentration, n/s = non-significant, * = $P \leq 0.05$, ** = $P < 0.01$, and *** = $P < 0.001$.
675
676 **Figure 6.** Needle biochemical responses to the treatments in healthy seedlings. **A**)
677 Needle nitrogen (N) concentrations; **B**) carbon (C) concentrations; **C**) the C/N ratio of
678 needles; **D**) soluble sugar concentrations; **E**) starch concentrations; **F**) total non-
679 structural carbohydrate (TNC) concentrations. Non-structural carbohydrates (**D,E,F**)
680 were measured in g of glucose equivalents g^{-1} (w/w). White, 0T; light grey, 4T; dark
681 grey, 8T. The horizontal line of the boxplot represents the mean; the box edges indicate
682 the 25th and 75th percentiles; the whiskers display the minimum and maximum values; n
683 = 6. Different letters above boxplots denote significant differences across all treatments
684 ($P < 0.05$). T = growth temperature, CO_2 = growth CO_2 concentration, n/s = non-
685 significant, * = $P \leq 0.05$, ** = $P < 0.01$, and *** = $P < 0.001$.
686
687 **Figure 7.** Photosynthetic and respiration measurements were similar in healthy and
688 dying seedlings. Comparison of **A**) net CO_2 assimilation rate (A_{growth}), **B**) shoot dark
689 respiration rate ($R_{shoot\text{-}growth}$), **C**) the ratio of A_{growth} to $R_{shoot\text{-}growth}$ (A/R_{growth}), **D**) maximum
690 rate of electron transport ($J_{1200\text{-}growth}$), **E**) maximum rate of Rubisco carboxylation ($V_{cmax\text{-}growth}$), and **F**) the ratio of $J_{1200\text{-}growth}$ to $V_{cmax\text{-}growth}$ ($J_{1200}/V_{cmax\text{-}growth}$) between dying (grey)
692 and healthy (white) seedlings grown in the 8TAC treatment. The horizontal line of the
693 boxplot represents the mean; the box edges indicate the 25th and 75th percentiles; the
694 whiskers display the minimum and maximum values; n = 6. Different letters above
695 boxplots denote significant differences between groups ($P < 0.05$).

Figure 8. Needle carbon concentrations were lower in dying seedlings than in healthy seedlings, although other biochemical indicators were similar in both groups. Biochemical responses between dying (grey) and healthy (white) seedlings grown in the 8TAC treatment. **A**) Needle nitrogen (N) concentrations; **B**) carbon (C) concentrations; **C**) the C/N ratio of needles; **D**) soluble sugar concentrations; **E**) starch concentrations; **F**) total non-structural carbohydrate (TNC) concentrations. The horizontal line of the boxplot represents the mean; the box edges indicate the 25^{th} and 75^{th} percentiles; the whiskers display the minimum and maximum values; n = 6. Different letters above boxplots denote significant differences between groups ($P < 0.05$).

Figure 9. Healthy seedlings had higher ratios of photosynthesis to respiration and higher leaf carbon concentrations than less healthy seedlings. Relationship between seedling health rating and **A**) the ratio of net CO_2 assimilation rate to shoot dark respiration rate at growth conditions (A/R_{growth}); and **B**) the percent needle carbon (%C). Points represent individual seedlings, n = 12. Solid line, linear regression.

Figures

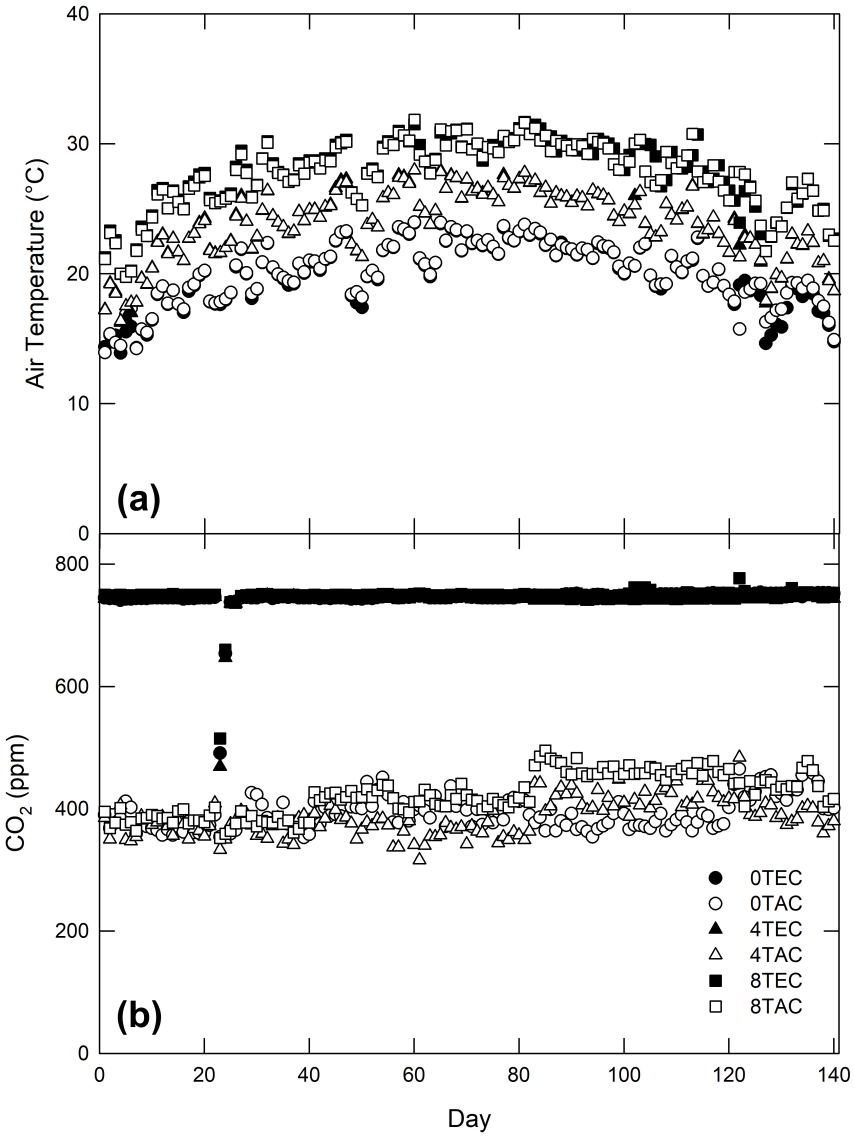

Figure 1. Daily temperature and CO_2 levels across all six glasshouses over the duration of the experiment. Day 0 indicates when seeds were potted (May 12th) and day 140 indicates when seedlings were harvested (Sept 28th). Temperature and CO_2 readings were taken daily at 12:00 am. Circles, ambient temperature (0T); triangles, +4 ˚C warming (4T); squares, +8 ˚C warming (8T). White symbols, ambient growth CO_2 (AC); black symbols, elevated growth CO_2 (EC).

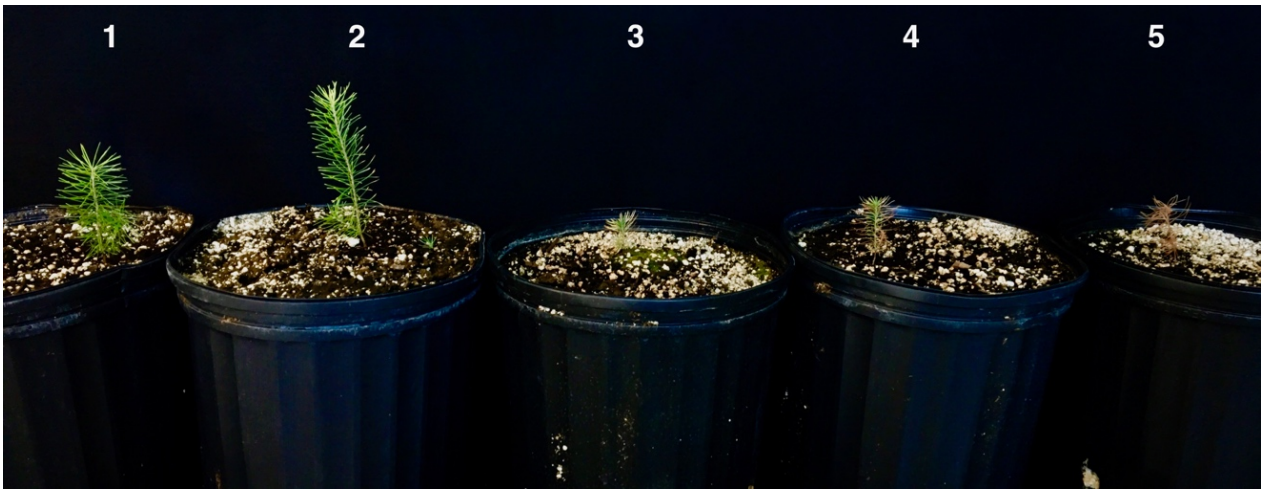

Figure 2. Representative seedlings showing the seedling health scale. (1) Needles are 100% green; (2) seedling has <50% brown needle tissue; (3) seedling has approximately 1:1 brown to green leaf tissue; (4) seedling has >50% brown needle tissue; (5) seedling is 100% brown.

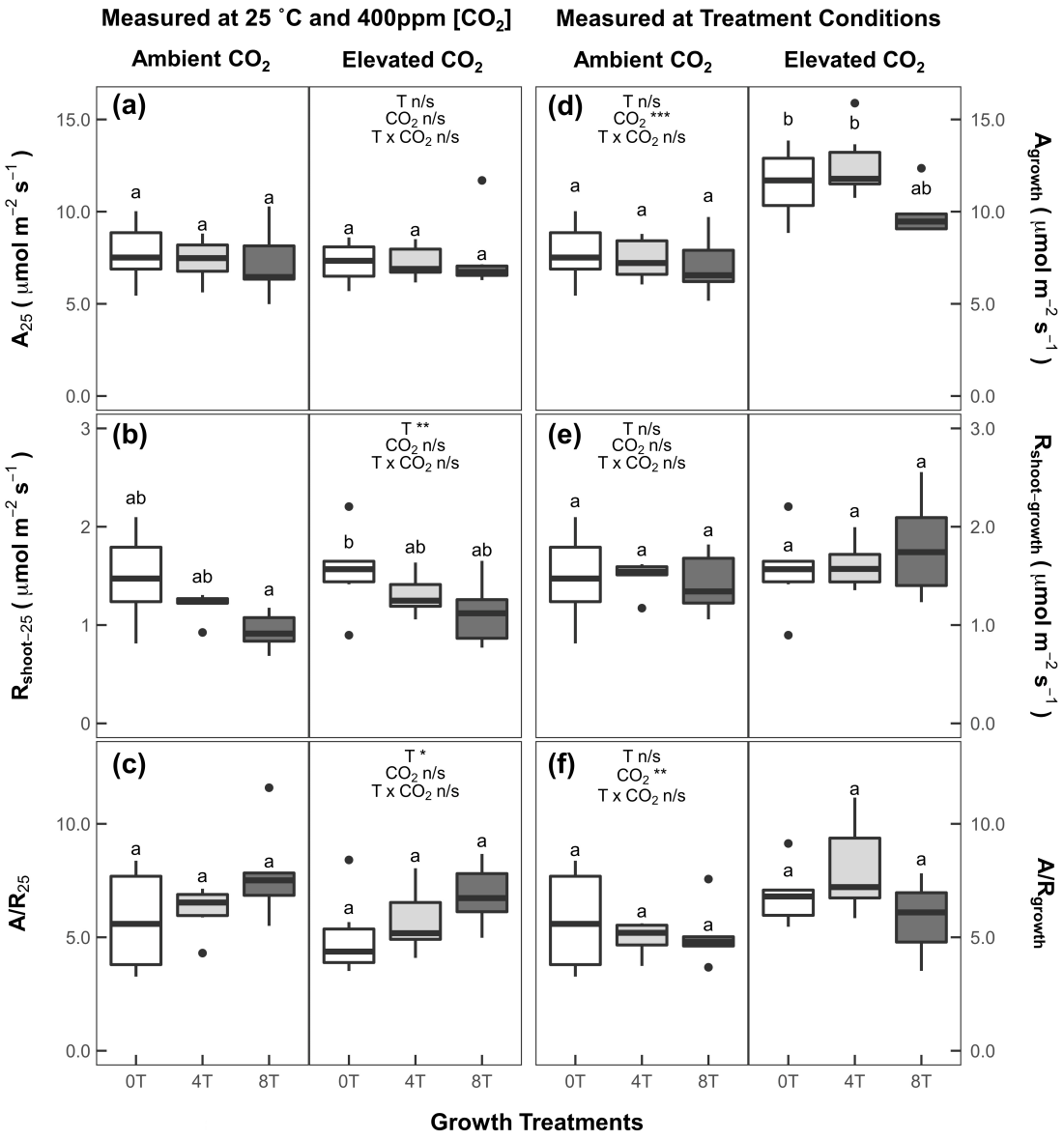

Figure 3. Thermal acclimation of respiration led to similar leaf carbon balances across the warming treatments, despite a lack of photosynthetic acclimation in healthy seedlings. Photosynthetic and respiratory responses to elevated CO_2 and temperature treatments measured at 25 ˚C and 400 ppm CO_2 (presented on the left) and growth conditions (25 ˚C for 0T, 29 ˚C for 4T, 33 ˚C for 8T; 400 ppm CO_2 for AC, 750 ppm CO_2 for EC) (presented on the right). **A, D)** net CO_2 assimilation rate (A_{25}, A_{growth}); **B, E)** shoot dark respiration rate ($R_{shoot-25}$, $R_{shoot-growth}$); **C, F)** the ratio of net CO_2 assimilation rate to respiration rate (A/R_{25}, A/R_{growth}). White, 0T; light grey, 4T; dark grey, 8T. The horizontal line of the boxplot represents the mean; the box edges indicate the 25th and 75th percentiles; the whiskers display the minimum and maximum values; n = 6. Different letters above boxplots denote significant differences across all treatments ($P < 0.05$). T = growth temperature, CO_2 = growth CO_2 concentration, n/s = non-significant, * = $P \leq 0.05$, ** = $P<0.01$, and *** = $P<0.001$.

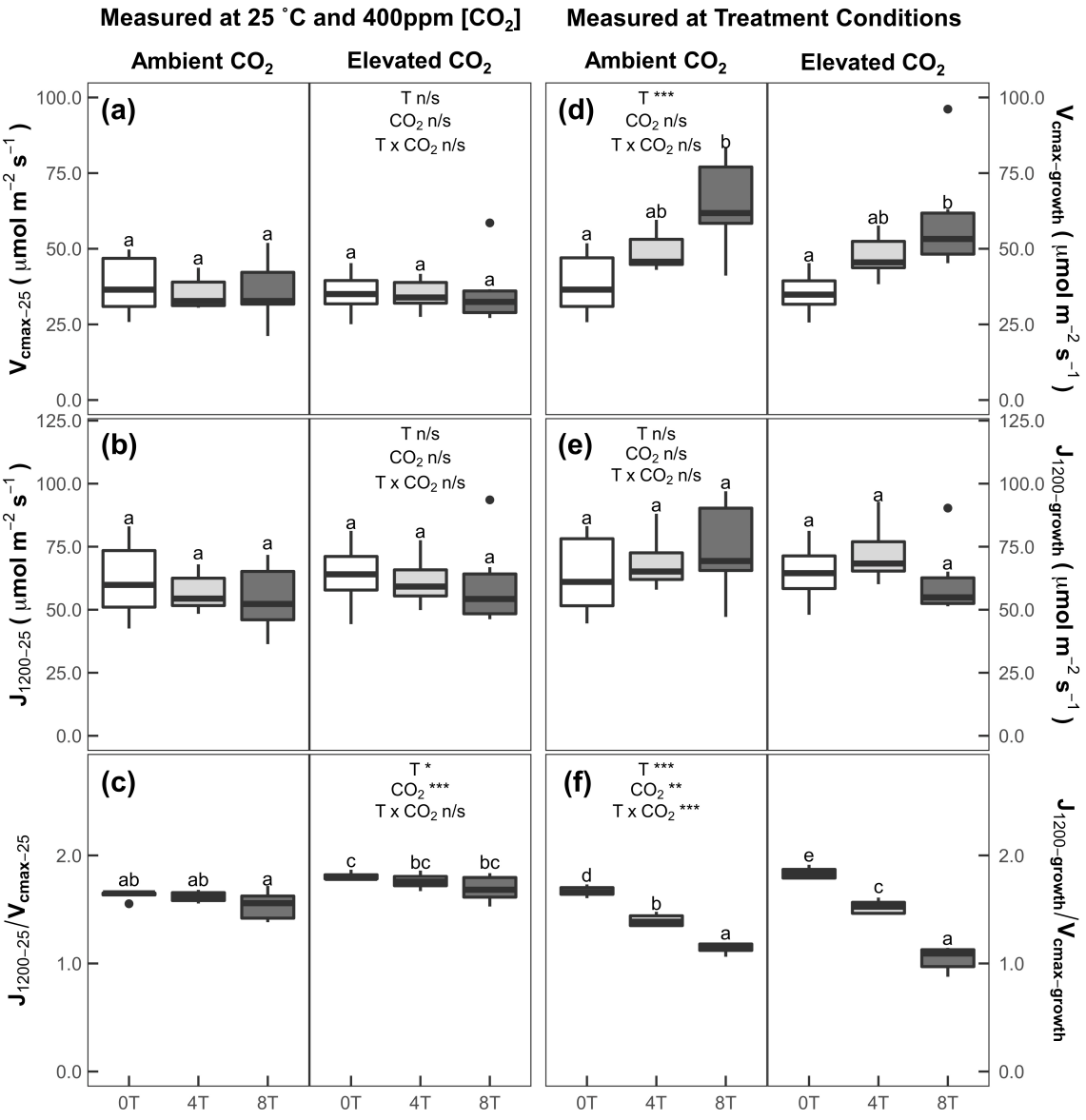

Figure 4. Photosynthetic capacity did not acclimate to either elevated CO_2 or warming in healthy seedlings. Responses of photosynthetic capacity at 25 ˚C and 400 ppm CO_2 (presented on the left) and growth conditions (25 ˚C for 0T, 29 ˚C for 4T, 33 ˚C for 8T; 400 ppm CO_2 for AC, 750 ppm CO_2 for EC) (presented on the right). (**A, D**) maximum rate of Rubisco carboxylation ($V_{cmax-25}$, $V_{cmax-growth}$); **B, E**) maximum rate of electron transport ($J_{1200-25}$, $J_{1200-growth}$); **C, F**) the ratio of J_{1200} to V_{cmax} ($J_{1200-25}/V_{cmax-25}$, $J_{1200-growth}/V_{cmax-growth}$). White, 0T; light grey, 4T; dark grey, 8T. The horizontal line of the boxplot represents the mean; the box edges indicate the 25th and 75th percentiles; the whiskers display the minimum and maximum values; n = 6. Different letters above boxplots denote significant differences across all treatments ($P < 0.05$). T = growth temperature, CO_2 = growth CO_2 concentration, n/s = non-significant, * = $P \leq 0.05$, ** = $P<0.01$, and *** = $P<0.001$.

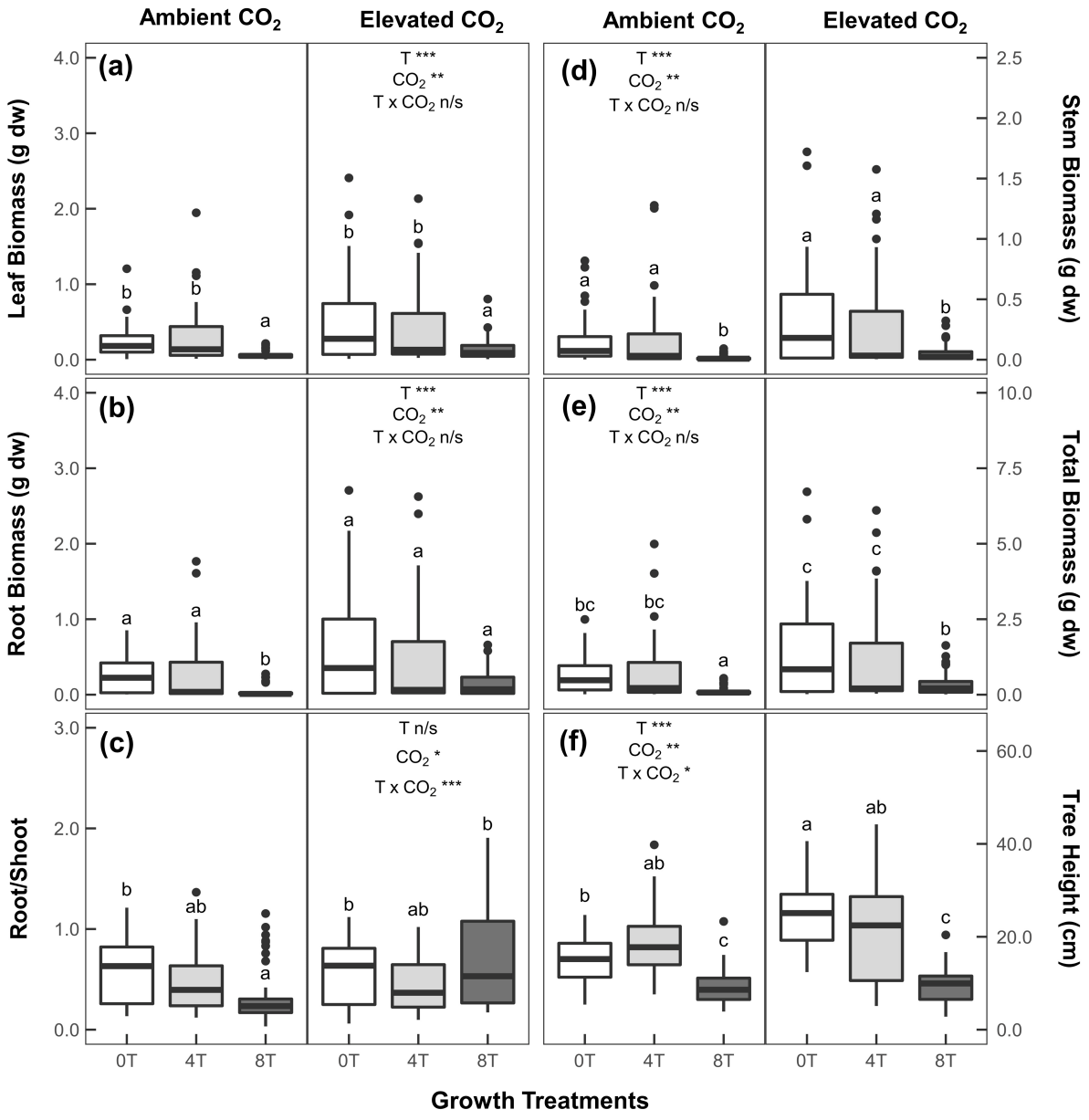

Figure 5. Warming suppressed seedling growth while high CO_2 stimulated growth in healthy seedlings. Growth responses to treatments**: A)** Leaf biomass**; B)** root biomass; **C)** the root/shoot ratio; **D)** stem biomass; **E)** total biomass; and **F)** tree height. White, 0T; light grey, 4T; dark grey, 8T. The horizontal line of the boxplot represents the mean; the box edges indicate the 25th and 75th percentiles; the whiskers display the minimum and maximum values; n = 40. Different letters above boxplots denote significant differences across all treatments ($P < 0.05$). T = growth temperature, CO_2 = growth CO_2 concentration, n/s = non-significant, * = $P \leq 0.05$, ** = $P<0.01$, and *** = $P<0.001$.

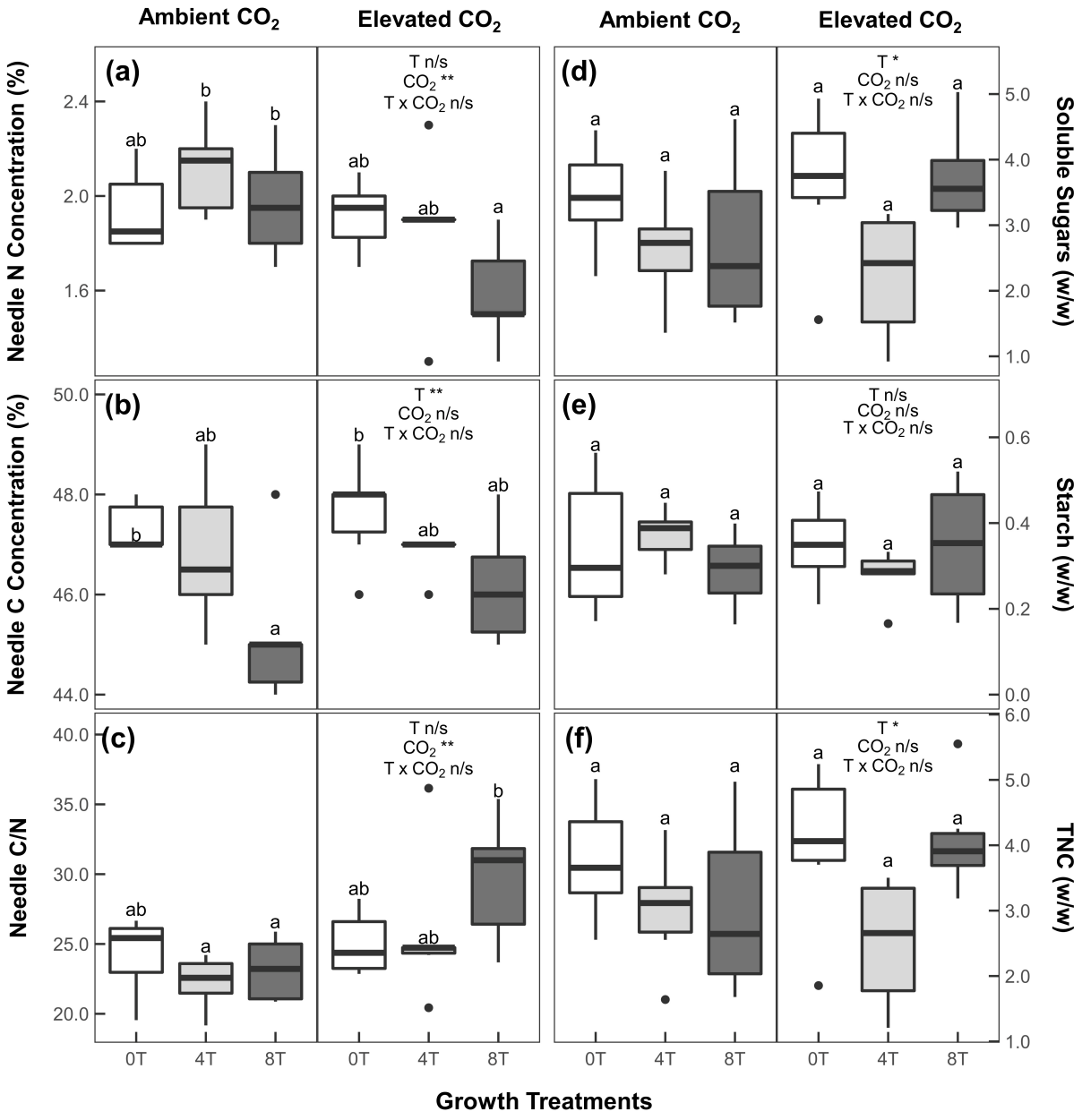

Figure 6. Needle biochemical responses to the treatments in healthy seedlings. **A**) Needle nitrogen (N) concentrations; **B**) carbon (C) concentrations; **C**) the C/N ratio of needles; **D**) soluble sugar concentrations; **E**) starch concentrations; **F**) total non-structural carbohydrate (TNC) concentrations. Non-structural carbohydrates (**D,E,F**) were measured in g of glucose equivalents g^{-1} (w/w). White, 0T; light grey, 4T; dark grey, 8T. The horizontal line of the boxplot represents the mean; the box edges indicate the 25th and 75th percentiles; the whiskers display the minimum and maximum values; n = 6. Different letters above boxplots denote significant differences across all treatments ($P < 0.05$). T = growth temperature, CO_2 = growth CO_2 concentration, n/s = non-significant, * = $P \leq 0.05$, ** = $P<0.01$, and *** = $P<0.001$.

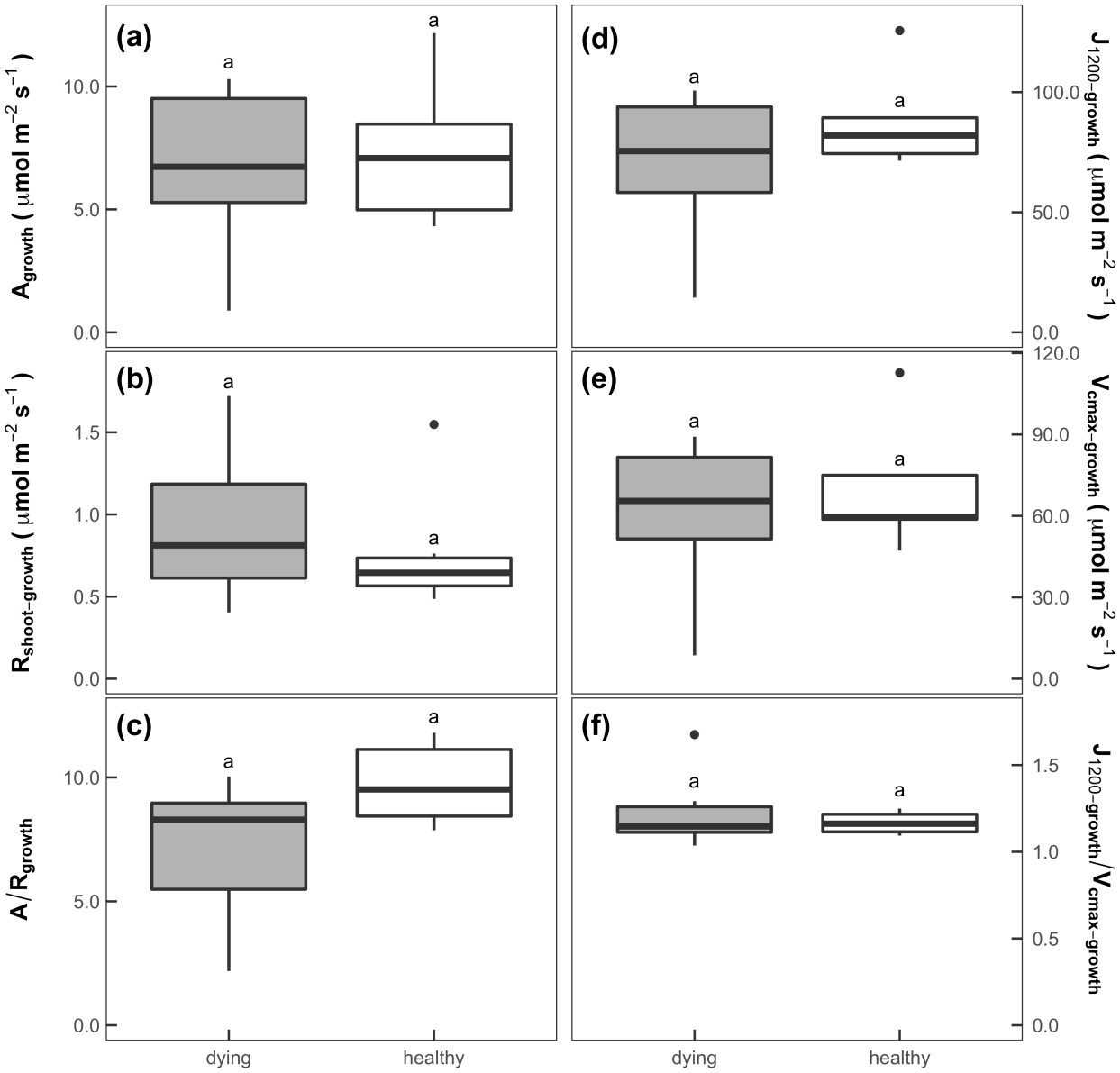

771

772 **Figure 7.** Photosynthetic and respiration measurements were similar in healthy and dying seedlings.
773 Comparison of **A**) net CO_2 assimilation rate (A_{growth}), **B**) shoot dark respiration rate ($R_{shoot-growth}$), **C**) the ratio of
774 A_{growth} to $R_{shoot-growth}$ (A/R_{growth}), **D**) maximum rate of electron transport ($J_{1200-growth}$), **E**) maximum rate of Rubisco
775 carboxylation ($V_{cmax-growth}$), and **F**) the ratio of $J_{1200-growth}$ to $V_{cmax-growth}$ ($J_{1200}/V_{cmax-growth}$) between dying (grey) and
776 healthy (white) seedlings grown in the 8TAC treatment. The horizontal line of the boxplot represents the mean;
777 the box edges indicate the 25th and 75th percentiles; the whiskers display the minimum and maximum values; n
778 = 6. Different letters above boxplots denote significant differences between groups ($P < 0.05$).

779

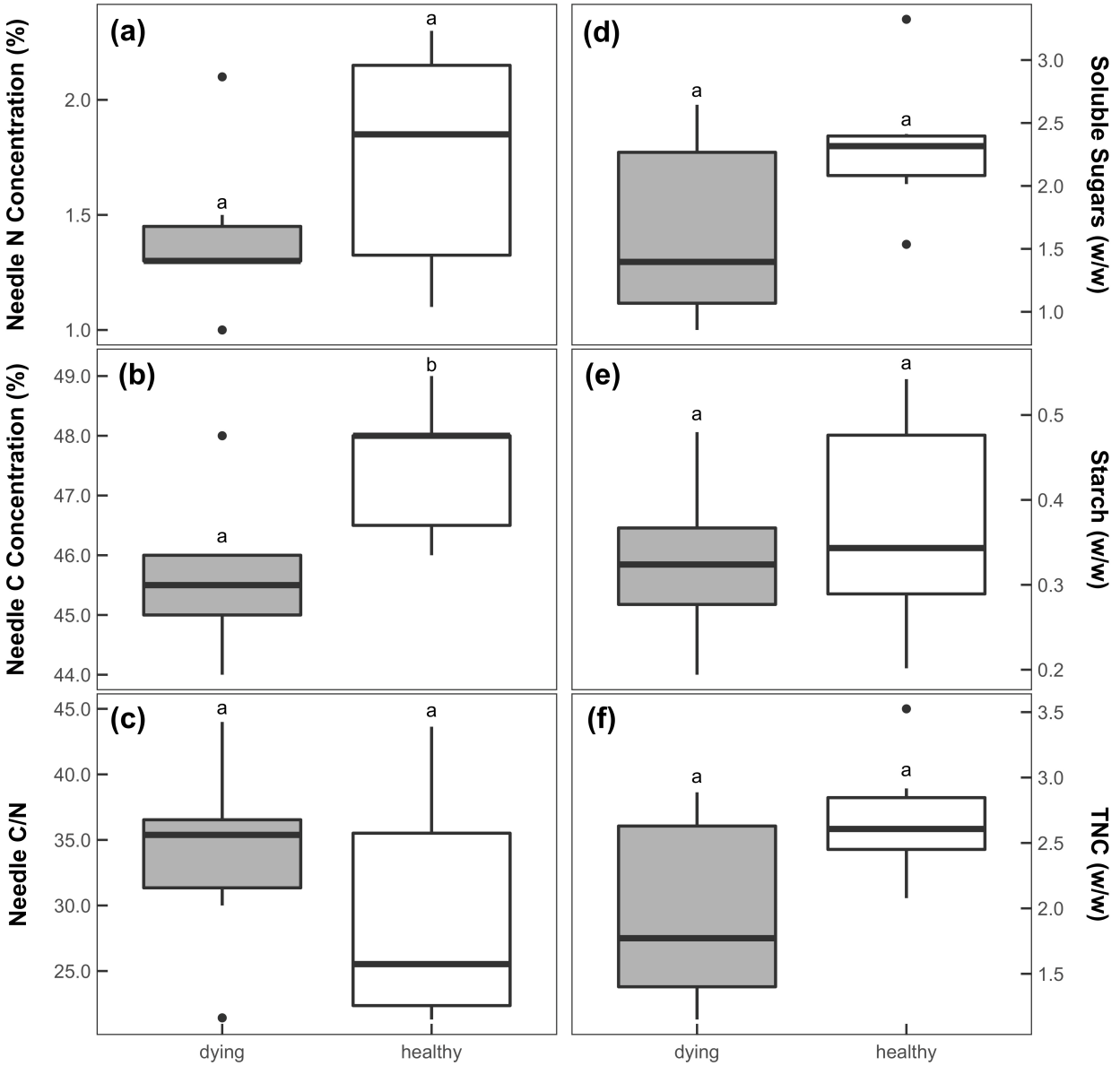

Figure 8. Needle carbon concentrations were lower in dying seedlings than in healthy seedlings, although other biochemical indicators were similar in both groups. Biochemical responses between dying (grey) and healthy (white) seedlings grown in the 8TAC treatment. **A**) Needle nitrogen (N) concentrations; **B**) carbon (C) concentrations; **C**) the C/N ratio of needles; **D**) soluble sugar concentrations; **E**) starch concentrations; **F**) total non-structural carbohydrate (TNC) concentrations. The horizontal line of the boxplot represents the mean; the box edges indicate the 25th and 75th percentiles; the whiskers display the minimum and maximum values; n = 6. Different letters above boxplots denote significant differences between groups ($P < 0.05$).

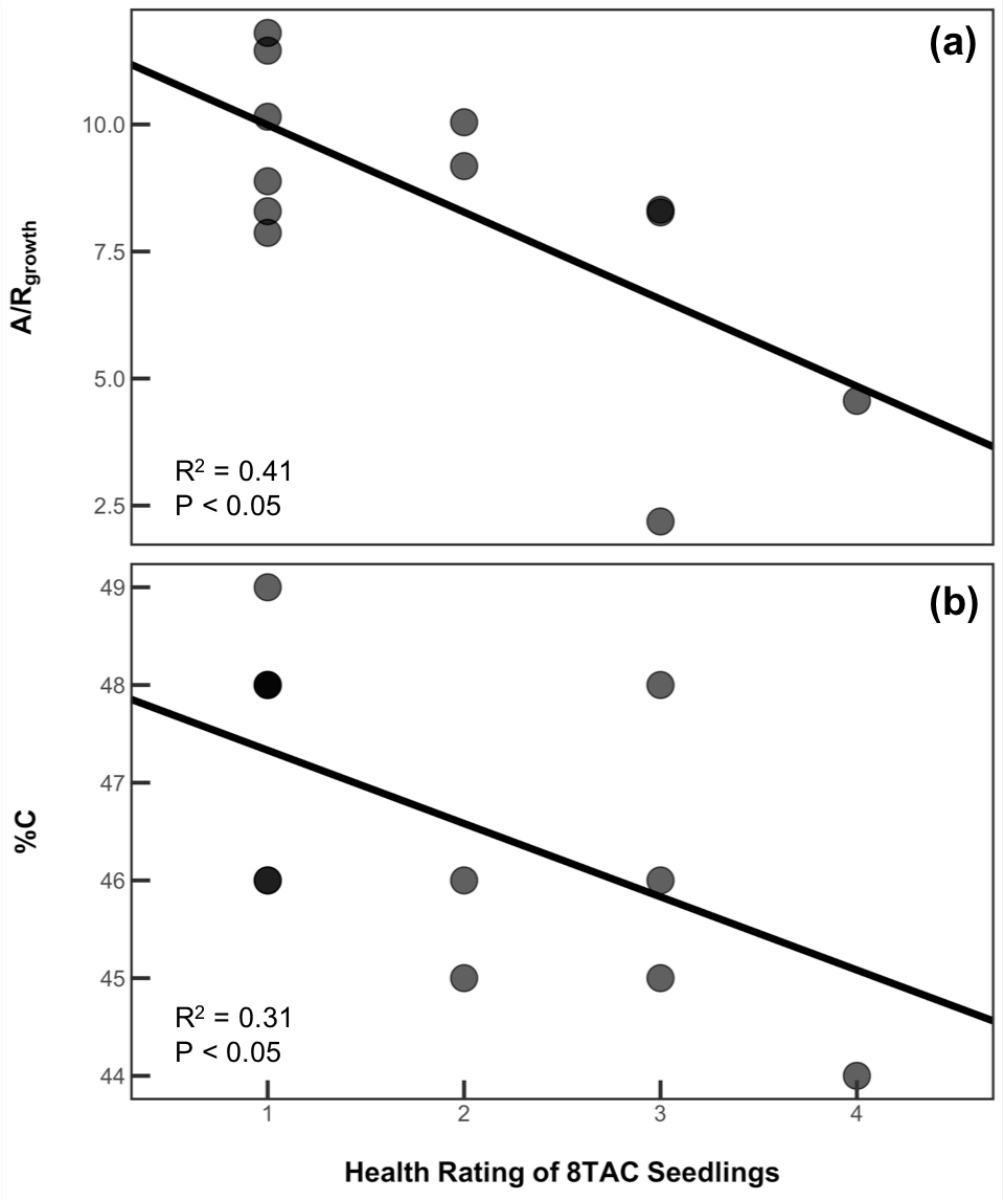

Figure 9. Healthy seedlings had higher ratios of photosynthesis to respiration and higher leaf carbon concentrations than less healthy seedlings. Relationship between seedling health rating and **A**) the ratio of net CO_2 assimilation rate to shoot dark respiration rate at growth conditions (A/R_{growth}); and **B**) the percent needle carbon (%C). Points represent individual seedlings, n = 12. Solid line, linear regression.

Supplementary Figures

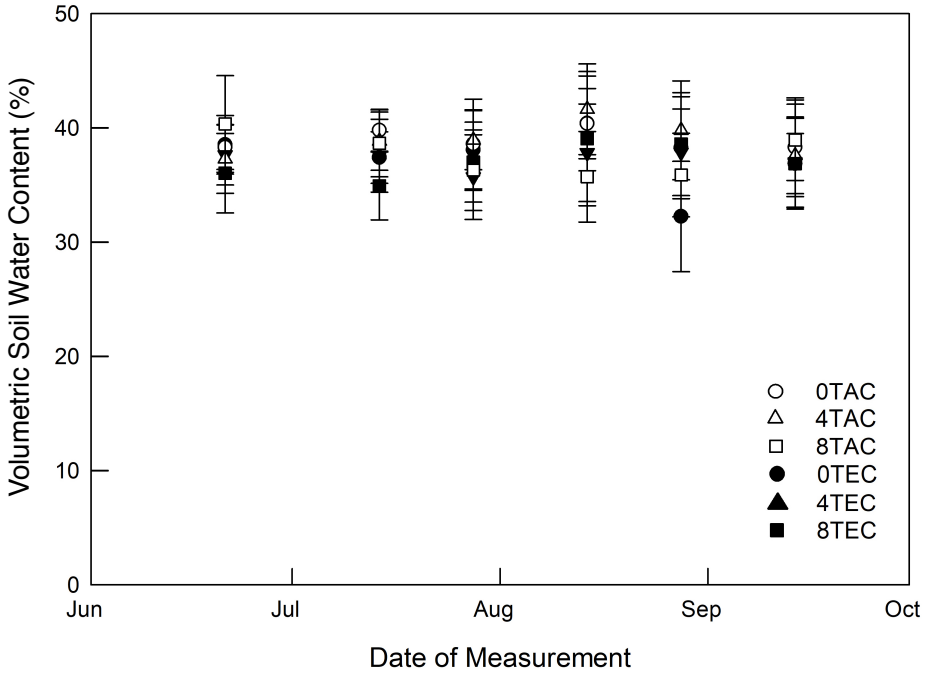

Figure S1. Volumetric soil water content (%) of tamarack seedlings grown under six climate treatments. Means ± SD, n = 40. Circles, ambient temperature (0T); triangles, +4 ˚C warming (4T); squares, +8 ˚C warming (8T). White symbols, ambient growth CO_2 (AC); black symbols, elevated growth CO_2 (EC).

References

Adams HD et al. (2017). A multi-species synthesis of physiological mechanisms in drought-induced tree mortality. Nat Ecol Evol 1:1285–1291.

Ainsworth EA, Long SP (2005) What have we learned from 15 years of free-air CO_2 enrichment (FACE)? A meta-analytic review of the responses of photosynthesis, canopy properties and plant production to rising CO_2. New Phytol 165:351–372.

Ainsworth EA, Rogers A (2007) The response of photosynthesis and stomatal conductance to rising [CO_2]: Mechanisms and environmental interactions. Plant Cell Environ 30:258–270.

Albert KR, Mikkelsen TN, Michelsen A, Ro-Poulsen H, van der Linden L (2011) Interactive effects of drought, elevated CO_2 and warming on photosynthetic capacity and photosystem performance in temperate heath plants. J Plant Physiol 16:1550–1561.

Allen CD et al. (2010) A global overview of drought and heat-induced tree mortality reveals emerging climate change risks for forests. For Ecol Manag 259:660–684.

Allen CD, Breshears DD, McDowell NG (2015) On underestimation of global vulnerability to tree mortality and forest die-off from hotter drought in the Anthropocene. Ecosphere 6:1–55.

Amthor JS, Koch GW, Willms JR, Layzell DB (2001) Leaf O_2 uptake in the dark is independent of coincident CO_2 partial pressure. J Ex Bot 52:2235–2238.

Anderegg WRL, Berry JA, Field CB (2012) Linking definitions, mechanisms, and modeling of drought-induced tree death. Trends Plant Sci 17:693–700.

Atkin OK, Tjoelker MG (2003) Thermal acclimation and the dynamic response of plant

840 respiration to temperature. Trends Plant Sci 8:343–351.
841 Bernacchi CJ, Singsaas EL, Pimental C, Portis AR Jr, Long SP (2001) Improved
842 temperature response functions for models of Rubisco-limited photosynthesis.
843 Plant Cell Environ 24:253–259.
844 Brandt, JP (2009) The extent of the North American boreal zone. Environ Rev 17:101–
845 161.
846 Cramer W et al. (2014). Detection and attribution of observed impacts. In: Field CB et
847 al. (eds), Climate Change 2014: Impacts, Adaptation, and Vulnerability. Part A:
848 Global and Sectoral Aspects. Contribution of Working Group II to the Fifth
849 Assessment Report of the Intergovernmental Panel of Climate Change. Cambridge,
850 United Kingdom and New York, NY, USA: Cambridge University Press. pp 979–
851 1037.
852 Crous KY, Walters MB, Ellsworth DS (2008) Elevated CO_2 concentration affects leaf
853 photosynthesis-nitrogen relationships in *Pinus taeda* over nine years in FACE. Tree
854 Physiol 28:607-614.
855 Davey PA, Hunt S, Hymus GJ, DeLucia EH, Drake BG, Karnosky DF, Long SP (2004)
856 Respiratory oxygen uptake Is not decreased by an instantaneous elevation of
857 [CO_2], but is increased with long-term growth in the field at elevated [CO_2]. Plant
858 Physiol 134:520-527.
859 DeLucia EH, Hamilton JG, Naidu SL, Thomas RB, Andrews JA, Finzi A, Lavine M,
860 Matamala R, Mohan JE, Hendrey GR, Schlesinger WH (1999) Net primary
861 production of a forest ecosystem with experimental CO_2 enrichment. Science
862 284:1177–1179.

863 Depardieu C, Girardin MP, Nadeau S, Lenz P, Bousquet J, & Isabel N. (2020). Adaptive
864 genetic variation to drought in a widely distributed conifer suggests a potential for
865 increasing forest resilience in a drying climate. New Phytol.
866 https://doi.org/10.1111/nph.16551
867 Dessler AE, Sherwood SC (2009) A matter of humidity. Science 303:1020–1021.
868 Dietze MC, Sala A, Carbone MS, Czimczik CI, Mantooth JA, Richardson AD, Vargas R
869 (2014) Nonstructural carbon in woody plants. Annu Rev Plant Biol 65:667–687.
870 Drake BG, Gonzàlez-Meler MA, Long SP (1997) More efficient plants: a consequence
871 of rising atmospheric CO_2? Annu Rev Plant Physiol Plant Mol Biol 48:609–639.
872 Du Y, Lu R, Xia J (2020) Impacts of global environmental drivers on non-structural
873 carbohydrates in terrestrial plants. Funct Ecol https://doi.org/10.1111/1365-
874 2435.13577
875 Dusenge ME, Madhavji S, Way DA (2020) Contrasting acclimation responses to
876 elevated CO_2 and warming between an evergreen and a deciduous boreal conifer.
877 Glob Change Biol https://doi.org/10.1111/gcb.15084
878 Dusenge ME, Ward EJ, Warren JM, Stinziano JR, Wullschleger SD, Hanson PJ, Way
879 DA (2021) Warming induces divergent stomatal dynamics in co-occurring boreal trees.
880 Glob Chang Biol. https://doi.org/10.1111/gcb.15620
881 Duursma R (2015) Plantecophys - an R package for analysing and modelling leaf gas
882 exchange data. PLoS ONE 10: e0143346.
883 Duursma R (2018) Plantecophys: Modelling and analysis of leaf gas exchange data. R
884 Package Version 1.4.4.
885 Ellsworth DS (1999) CO_2 enrichment in a maturing pine forest: are CO_2 exchange and

886 water status in the canopy affected? Plant Cell and Environ 22:461–472
887 Farquhar GD, von Caemmerer S, Berry JA (1980) A biochemical model of
888 photosynthetic CO_2 assimilation in leaves of C_3 species. Planta 149:78–90.
889 Gower ST, Richards JH (1990) Larches: Deciduous conifers in an evergreen world.
890 BioScience 40(11): 818–826. https://doi.org/10.2307/1311484
891 Hartmann H et al. (2018) Research frontiers for improving our understanding of drought-
892 induced tree and forest mortality. New Phytol 218:15–28.
893 Hartmann H, Trumbore S (2016) Understanding the roles of nonstructural
894 carbohydrates in forest trees - from what we can measure to what we want to
895 know. New Phytol 211:386–403.
896 Haworth M, Moser G, Raschi A, Kammann C, Grunhage L, Muller C (2016) Carbon
897 dioxide fertilisation and supressed respiration induce enhanced spring biomass
898 production in a mixed species temperate meadow exposed to moderate carbon
899 dioxide enrichment. Funct Plant Biol 43:26–39.
900 Hikosaka K, Ishikawa K, Borjigidai A, Muller O, Onoda Y (2006) Temperature
901 acclimation of photosynthesis: Mechanisms involved in the changes in temperature
902 dependence of photosynthetic rate. J Ex Bot 57:291–302.
903 Hoch G, RIchter A, Korner Ch (2003) Non-structural carbon compounds in temperate
904 forest trees. Plant Cell Environ 26:1067-1081
905 Islam MA, Macdonald SE (2004) Ecophysiological adaptations of black spruce (*Picea*
906 *mariana*) and tamarack (*Larix laricina*) seedlings to flooding. Trees-Struct Funct
907 18:35–42.
908 Jauregui I, Apaircio-Tejo PM, Avila C, Rueda-Lopez M, Arenjuelo I (2015) Root and

shoot performance of *Arabidposis thaliana* exposed to elevated CO_2: A physiologic, metabolic, and transcriptomic response. J Plant Physiol 189:65–76.

Kattge J, Knorr W (2007) Temperature acclimation in a biochemical model of photosynthesis: A reanalysis of data from 36 species. Plant Cell Environ 30:1176–1190.

Kattge J, Knorr W, Raddatz T, Wirth C (2009) Quantifying photosynthetic capacity and its relationship to leaf nitrogen content for global-scale terrestrial biosphere models. Glob Change Biol 15:976–991.

Kloeppel BD, Gower ST, Vogel JG, Reich PB (2000) Leaf-level resource use for evergreen and deciduous conifers along a resource availability gradient. Funct Ecol 14(3): 281–292. https://doi.org/10.1046/j.1365-2435.2000.00439.x

Kroner Y, Way DA (2016) Carbon fluxes acclimate more strongly to elevated growth temperatures than to elevated CO_2 concentrations in a northern conifer. Glob Change Biol 22:2913–2928.

Kurepin LV, Stangl ZR, Ivanov AG, Bui V, Mema M, Hüner NPA, Oquist G, Way D, Hurry V (2018) Contrasting acclimation abilities of two dominant boreal conifers to elevated CO_2 and temperature. Plant Cell Environ 41:1331–1345.

Landhäusser SM et al (2018) Standardized protocols and procedures can precisely and accurately quantify non-structural carbohydrates. Tree Physiol 38:1764–1778.

Leakey ADB, Ainsworth EA, Bernacchi CJ, Roger A, Long SP, Ort DR (2009) Elevated CO_2 effects on plant carbon, nitrogen, and water relations: Six important lessons from FACE. J Ex Bot 60:2859–2876.

Lenth RV, Buerkner P, Herve M, Love J, Riebl H, Singmann H (2021). emmeans:

932 estimated marginal means, aka least-squares. R package version 1.5.5-1
933 Lin Y, Medlyn BE, Ellsworth DS (2012). Temperature responses of leaf net
934 photosynthesis: the role of component processes. Tree Physiol 32:219–231.
935 Loveys BR, Atkinson LJ, Sherlock DJ, Roberts RL, Fitter AH, Atkin OK (2003) Thermal
936 acclimation of leaf and root respiration: An investigation comparing inherently fast-
937 and slow-growing plant species. Glob Change Biol 9:895–910.
938 Luo Y, Chen HYH (2015) Climate change-associated tree mortality increases without
939 decreasing water availability. Ecol Lett 18:1207–1215.
940 Ma S, He F, Tian D, Zou D, Yan Z, Yang Y, Zhou T, Huang K, Shen H, Fang J (2018)
941 Variations and determinants of carbon content in plants: A global synthesis.
942 Biogeosciences 15:693–702.
943 Maire V, Martre P, Kattge J, Gastal F, Esser G, Fontaine S, Soussana JF (2012) The
944 coordination of leaf photosynthesis links C and N fluxes in C_3 plant species. PLoS
945 ONE 7:1–15.
946 McDermid J, Fera S, Hogg A (2014) Climate change projections for Ontario: An
947 updated synthesis for policymakers and planners. Ontario Ministry of Natural
948 Resources
949 Mcdowell NG, Sevanto S (2010) The mechanisms of carbon starvation: how, when, or
950 does it even occur at all? New Phytol 186:264–266.
951 Medlyn BE, Barton CVM, Broadmeadow MSJ, Ceulemans R, De Angelis P, Forstreuter
952 M, Freeman M, Jackson SB, Kellomaki S, Laitat E, Rey A, Roberntz P, Sigurdsson
953 BD, Strassemeyer J, Wang K, Curtis PS, Jarvis PG (2001) Stomatal conductance
954 of forest species after long-term exposure to elevated CO_2 concentration: A

955 synthesis. New Phytol 149:247–264.
956 Medlyn BE, Dreyer E, Ellsworth D, Forstreuter M, Harley PC, Kirschbaum MUF, Le
957 Roux X, Montpied P, Strassemeyer J, Walcroft A, Wang K, Loustau D (2002)
958 Temperature response of parameters of a biochemical based model of
959 photosynthesis. II. A review of experimental data. Plant Cell Environ 25:1167–1179.
960 Moore BD, Cheng SH, Sims D, Seemann JR (1999) The biochemical and molecular
961 basis for photosynthetic acclimation to elevated atmospheric CO_2. Plant Cell
962 Environ 22:567–582.
963 Onoda Y, Hikosaka K, Hirose T (2005) Seasonal change in the balance between
964 capacities of RuBP carboxylation and RuBP regeneration affects CO_2 response of
965 photosynthesis in *Polygonum cuspidatum.* J Ex Bot 56:755–763.
966 Oppenheimer M, Campos M, Warren R, Birkmann J, Luber G, O'Neill BC, Takahashi K
967 (2014) Emergent risks and key vulnerabilities. In: CB Field et al. (eds), *Climate*
968 *Change 2014: Impacts, Adaptation, and Vulnerability. Part A: Global and Sectoral*
969 *Aspects. Contribution of Working Group II to the Fifth Assessment Report of the*
970 *Intergovernmental Panel of Climate Change.* Cambridge, United Kingdom and New
971 York, NY, USA: Cambridge University Press. pp 1039–1099
972 Peng C, Ma Z, Lei X, Zhu Q, Chen H, Wang W, Liu S, Weizhong L, Fang X, Zhou, X
973 (2011) A drought-induced pervasive increase in tree mortality across Canada's
974 boreal forests. Nat Clim Change 1:467–471.
975 Pinheiro J, Bates D, DebRoy S, Sarkar D, R Development Core Team (2013). nlme:
976 linear and non-linear mixed effect models. R package version 3.1-108.
977 Poorter H, Niklas KJ, Reich PB, Oleksyn J, Poot P, Mommer L (2012) Biomass

allocation to leaves, stems and roots: Meta-analyses of interspecific variation and environmental control. New Phytol 193:30–50.

Reich PB, Walters MB, Ellsworth DS, Vose JM, John C, Gresham C, Bowman WD (1998) Relationships of leaf dark respiration to leaf nitrogen, specific leaf area and leaf life- span: A test across biomes and functional groups. Oecol 114:471–482.

Ryan MG (2013). Three decades of research at Flakaliden advancing whole-tree physiology, forest ecosystem and global change research. Tree Physiol 33:1123–1131.

Sage RF, Kubien DS (2007) The temperature response of C_3 and C_4 photosynthesis. Plant Cell Environ 30:1086–1106.

Serreze MC, Walsh JE, Chapin FSI, Osterkamp T, Dyurgerov M, Romanovsky V, Oechel WC, Morison J, Zhang T, Barry RG (2000) Observational evidence of recent change in the northern high-latitude environment. Clim Change 46:159–207.

Sevanto S, Mcdowell NG, Dickman LT, Pangle R, Pockman WT (2014) How do trees die? A test of the hydraulic failure and carbon starvation hypotheses. Plant Cell Environ 37:153–161.

Slot M, Kitajima K. (2015). General patterns of acclimation of leaf respiration to elevated temperatures across biomes and plant types. Oecol 177:885–900.

So WK, Yiotis C, Murray M, Parnell A, Wright IJ, Spicer RA, Lawson T, Caballero R, McElwain JC (2019) Rising CO_2 drives divergence in water use efficiency of evergreen and deciduous plants. Sci Adv. https://doi.org/10.1126/sciadv.aax7906

Taub DR, Wang X (2008) Why are nitrogen concentrations in plant tissues lower under elevated CO_2? A critical examination of the hypotheses. J Integr Plant Biol

50:1365–1374.

Tissue DT, Lewis JD, Wullschleger SD, Amthor JS, Griffin KL, Anderson OR (2001) Leaf respiration at different canopy positions in sweetgum (*Liquidambar styraciflua)* grown in ambient and elevated concentrations of carbon dioxide in the field. Tree Physiol 22:1157-1166.

Tjoelker MG, Oleksyn J, Reich PB (1998) Seedlings of five boreal tree species differ in acclimation of net photosynthesis to elevated CO_2 and temperature. Tree Physiol 18:715–716.

Tjoelker MG, Oleksyn J, Reich P (1999a) Acclimation of respiration to temperature and CO_2 in seedlings of boreal tree species in relation to plant size and relative growth rate. Glob Change Biol 49:679–691.

Tjoelker MG, Reich PB, Oleksyn J (1999b) Changes in leaf nitrogen and carbohydrates underlie temperature and CO_2 acclimation of dark respiration in five boreal species. Plant Cell Envion 22:767-778

Togashi FH, Prentice CI, Atkin OK, Macfarlane C, Prober SM, Bloomfield KJ, Evans BJ (2018) Thermal acclimation of leaf photosynthetic traits in an evergreen woodland, consistent with the coordination hypothesis. Biogeosciences 15:3461–3474.

Trenberth KE (2011) Changes in precipitation with climate change. Clim Res *47*:123–138.

Way DA, Oren R (2010) Differential responses to changes in growth temperature between trees from different functional groups and biomes: A review and synthesis of data. Tree Physiol 30:669–688.

Way DA, Oren R, Kroner Y (2015) The space-time continuum: The effects of elevated

1024 CO_2 and temperature on trees and the importance of scaling. Plant Cell Environ
1025 38:991–1007.
1026 Way DA, Yamori W (2014) Thermal acclimation of photosynthesis: On the importance of
1027 adjusting our definitions and accounting for thermal acclimation of respiration.
1028 Photosynth Res 119:89–100.
1029 Weber R, Gessler A, Hoch G (2019) High carbon storage in carbon-limited trees. New
1030 Phytol 222:171-182
1031 Wickham H (2017) Tidyverse. R Package Version 1.2.0
1032 Wiley E, Hoch G, Landhäusser SM (2017) Dying piece by piece: Carbohydrate
1033 dynamics in aspen (*Populus tremuloides*) seedlings under severe carbon stress. J
1034 Ex Bot 68:5221–5232.
1035 Yamori W, Hikosaka K, Way DA (2014) Temperature response of photosynthesis in C_3,
1036 C_4, and CAM plants: Temperature acclimation and temperature adaptation.
1037 Photosynth Res 119:101–117.
1038 Yamori W, Noguchi K, Terashima I (2005) Temperature acclimation of photosynthesis in
1039 spinach leaves: Analyses of photosynthetic components and temperature
1040 dependencies of photosynthetic partial reactions. Plant Cell Environ 28:536–547.
1041 Yin HJ, Liu Q, Lai T (2008) Warming effects on growth and physiology in the seedlings
1042 of the two conifers *Picea asperata* and *Abies faxoniana* under two contrasting light
1043 conditions. Ecol Res 23:459–469.
1044 Yin X (2002) Responses of leaf nitrogen concentration and specific leaf area to
1045 atmospheric CO_2 enrichment: A retrospective synthesis across 62 species. Glob
1046 Change Biol 8:631–642.

1047 Zhang S, Tao F, Zhang Z (2017) Spatial and temporal changes in vapour pressure
1048 deficit and their impacts on crop yields in China during 1980-2008. J Meteorol Res
1049 31:800–808.